

## Chapter 2

# Topological Solid State Systems: Conjectures, Experiments and Models

**Abstract** This chapter reviews the ten classes of topological insulators and superconductors and presents their classifying table. The two complex classes of the table, which are the focus of our work, are then discussed in depth. The emphasis is on the physical properties, experimental achievements and the conjectures put forward by the physics community. The bulk-boundary correspondence principle is exemplified using exactly solvable models in arbitrary dimensions. The chapter also introduces the generic classes of physical models which incorporate the effect of an external magnetic field and disorder. It elaborates the main assumptions and summarizes the behavior of various physical quantities of interest. The reader will find here several technical results from functional analysis used in our work.

### 2.1 The Classification Table

Hereafter, a crystal will be said to be insulating in the bulk if the direct bulk resistivity diverges as the temperature is taken to zero. In what concerns the electron-electron interaction, all insulators mentioned in this work are well described by mean-field approximations, hence the analysis is always carried out in the independent electron picture. Then, a strong topological insulator is a crystal which is insulating in the bulk, but becomes metallic when an edge or a surface (called boundary hereafter) is cut to the crystal. This definition automatically implies that boundary spectrum emerges at the Fermi level and, since disorder is unavoidable in real samples, it also implies that this spectrum is immune to Anderson localization, at least in the regime of weak disorder. For superconductors, the fermionic quasiparticle excitations are assumed to be well described within the Bogoliubov-de Gennes approximation. Then a strong topological superconductor has gapped fermionic quasiparticle excitations in the bulk, but supports gapless excitations modes along any boundary cut to the system. There are other effects appearing in topological insulators, e.g. the existence of zero modes attached to defects, but this is not in the focus of the present work (except in Chap. 1).

One of the first efforts to classify the strong topological insulators and superconductors was undertaken by Schnyder, Ryu, Furusaki, and Ludwig in [192]. The first

accomplishment of their work was to realize that the classification should be performed inside the universality classes. Focussing mainly on random matrices, Altland and Zirnbauer [5, 232] argued that there are ten classes which cover both Fermionic systems of electrons with conserved particle number and systems of the Bogoliubov-de Gennes type. These classes are listed in Table 2.1. Each class is characterized by the transformations of their elements, i.e. the quantum systems themselves, under three generic symmetries, namely, the time-reversal (TRS), particle-hole (PHS) and chiral (CHS) symmetries. The TRS and PHS can square to plus or minus the identity, leading to a total of precisely ten distinct choices. Note that the combination of a TRS and a PHS results in a transformation of CHS type, and this aspect needs to be taken into account when counting the universality classes. As explained in Ref. [232], these classes are closely connected to Cartan's symmetric spaces, which explains the Cartan labels assigned to them (e.g. A, AIII, etc.). The separation in universality classes applies to random matrices and disordered metals and insulators alike. Ref. [192] then went systematically over these ten classes for bulk insulators in dimension  $d \leq 3$ , by performing an analysis of the localized/delocalized character of the boundary states in the presence of disorder. This analysis was based on the classification of the one- and two-dimensional disordered Dirac Hamiltonians by Bernard and LeClair [24] and on a complementary field-theoretic argument based on the replica trick, both of which rely on effective theories involving saddle-point approximations (the non-linear sigma models). The final conjecture of Ref. [192] was that all topological phases for  $d \leq 3$  (those with a non-vanishing entry in Table 2.1) display delocalized boundary spectrum which fills the bulk gap entirely. For the

**Table 2.1** Classification table of strong topological insulator and superconductors

$j$	TRS	PHS	CHS	CAZ	$d = 0, 8$	$d = 1$	$d = 2$	$d = 3$	$d = 4$	$d = 5$	$d = 6$	$d = 7$
0	0	0	0	A	$\mathbb{Z}$		$\mathbb{Z}$		$\mathbb{Z}$		$\mathbb{Z}$	
1	0	0	1	AIII		$\mathbb{Z}$		$\mathbb{Z}$		$\mathbb{Z}$		$\mathbb{Z}$
0	+1	0	0	AI	$\mathbb{Z}$				$2\mathbb{Z}$		$\mathbb{Z}_2$	$\mathbb{Z}_2$
1	+1	+1	1	BDI	$\mathbb{Z}_2$	$\mathbb{Z}$				$2\mathbb{Z}$		$\mathbb{Z}_2$
2	0	+1	0	D	$\mathbb{Z}_2$	$\mathbb{Z}_2$	$\mathbb{Z}$				$2\mathbb{Z}$	
3	-1	+1	1	DIII		$\mathbb{Z}_2$	$\mathbb{Z}_2$	$\mathbb{Z}$				$2\mathbb{Z}$
4	-1	0	0	AII	$2\mathbb{Z}$		$\mathbb{Z}_2$	$\mathbb{Z}_2$	$\mathbb{Z}$			
5	-1	-1	1	CII		$2\mathbb{Z}$		$\mathbb{Z}_2$	$\mathbb{Z}_2$	$\mathbb{Z}$		
6	0	-1	0	C			$2\mathbb{Z}$		$\mathbb{Z}_2$	$\mathbb{Z}_2$	$\mathbb{Z}$	
7	+1	-1	1	CI				$2\mathbb{Z}$		$\mathbb{Z}_2$	$\mathbb{Z}_2$	$\mathbb{Z}$

Each row represents a universal symmetry class, defined by the presence (1 or  $\pm 1$ ) or absence (0) of the three symmetries: time-reversal (TRS), particle-hole (PHS) and chiral (CHS), and by how TRS and PHS transformations square to either  $+1$  or  $-1$ . Each universality class is identified by a Cartan-Altland-Zirnbauer (CAZ) label. The strong topological phases are organized by their corresponding symmetry class and space dimension  $d = 0, \dots, 8$ . These phases are in one-to-one relation with the elements of the empty,  $\mathbb{Z}_2$ ,  $\mathbb{Z}$  or  $2\mathbb{Z}$  groups. The table is further divided into the complex classes A and AIII (top two rows), which are the object of the present study, and the real classes AI, ..., CI (the remaining 8 rows)

unitary chiral AIII class it is now known that the conjecture is not entirely true, as disorder can localize the entire boundary spectrum except at the Fermi level [65], which for AIII class is pinned at  $E = 0$ , and magnetic fields can even open spectral gaps in the boundary spectrum. Ref. [192] also introduced a higher winding number for chiral systems in dimension  $d = 3$  allowing to distinguish so-called strong topological insulators. The possible values of this invariant and its analogues in other dimensions and universality classes appear in Table 2.1. For example, the  $\mathbb{Z}$  for class A systems in  $d = 2$  is the well-known Chern number of quantum Hall systems.

The structure of the classifying table reported in Ref. [192] differed from the one seen in Table 2.1. The latter displays an obvious flow-pattern and periodicity with the space dimension and, because of these characteristics, the table is also called the periodic table of topological insulators and superconductors. These features were pointed out by Kitaev [115], who noted that the systems with (without) TRS and PHS are classified by the real (complex)  $K$ -theories. Then Bott periodicity alone can explain the patterns seen in Table 2.1, as it is nicely explained in Refs. [111, 143, 203, 207] for the real classes. See also [77] for an index-theoretic approach which holds in the regime of strong disorder. In the complex case, there are only two available  $K$ -groups, the  $K_0$  and  $K_1$  groups, and they classify the two complex classes A and AIII, respectively. One can move between the two groups using the suspensions maps, the  $\theta$ -map and the Bott map (see Sect. 4.1.4), which effectively increase the space dimension by one. As such, to any strong topological insulator from class A one can associate a strong topological insulator from class AIII using Bott map and by doubling the dimension of the fiber to accommodate for the chiral symmetry; and to each topological system from AIII class one can associate a strong topological insulator from class A using the  $\theta$ -map. Repeating this procedure, starting from  $d = 0$  where  $K_0 \simeq \mathbb{Z}$ , one can get an understanding of the flow-pattern, the periodicity and the counting of the strong complex topological phases listed in Table 2.1. Let us mention that Table 2.1 is adopted from Ref. [190], which relied on the same classifying criterion and methods as Ref. [192]. Further let us point out that the  $2\mathbb{Z}$  entries in Table 2.1 express that the invariants for the corresponding systems are always even [77, 190].

The complex  $K$ -groups of the algebras of bulk observables, in the presence of disorder and magnetic fields, are listed in Sect. 4.2 and, as one can immediately see from Table 2.1, the strong topological insulators account only for a fraction of these groups. As discussed in Sect. 4.2.3, the strong topological systems are generated by the top generators of the  $K$ -groups, while the rest of the generators generate the so-called weak topological insulators. The same is true for the real classes. An example of weak topological insulator is the quantum Hall effect in three space dimensions [120]. As we shall see, the bulk-boundary principle applies to the weak topological insulators too, but with two important modifications: (1) The principle does not work for all boundaries. In other words, boundaries cut along specific crystallographic planes do not carry topological boundary states (see [225] for explicit examples). (2) Their bulk and boundary invariants (see Sects. 5.3 and 5.2) do not satisfy index formulas and for this reason the bulk invariants cannot be formulated in the regime of strong disorder and the delocalization of the topological boundary spectrum cannot

be established by the present methods. The latter remains an important open issue because, in certain circumstances, the weak topological insulators were shown to display metallic boundary states in the presence of disorder [15, 118, 140, 186] and robust conducting channels along line-defects [93]. We want to mention that new mathematical tools, targeting precisely this issue, were put forward in Ref. [165].

Lastly, let us point out that there are additional classes of topological insulators which received substantial attention from both theoretical and experimental physics communities. These are the crystalline topological insulators [9, 69], which are stabilized by the TRS and a space point-symmetry of the crystal, and furthermore the spin-orbit and TRS free topological insulators [6], which are stabilized just by a space point-symmetry. By stabilized we mean that interesting topological classifications of phases emerges when these constraints are enforced, at least in the periodic case.

## 2.2 The Unitary Class

The systems in the unitary class have no symmetry constraints except for the requirement that the time evolution is unitary. As a consequence, the generators of the time evolution, which are the Hamiltonians if the discussion is about the quantum systems, are self-adjoint operators. This means, for example, that open or dissipative quantum systems are excluded from the unitary class or, putted differently, the topological characteristics associated with the unitary class may brake down when unitarity is lost. As such, the self-adjoint property of the Hamiltonians can be regarded as a “symmetry” which, like all the other symmetries in the classification table, stabilizes the topological properties of the systems from class A. In this section we introduce the models and their physical characteristics, both for bulk and half-space. We formulate the bulk-boundary principle for periodic systems and demonstrate this principle using an exactly solvable model in arbitrary dimensions. The existing experimental results are briefly surveyed.

### 2.2.1 General Characterization

The most general translation invariant (i.e. 1-periodic) lattice model from the unitary class in  $d$  space dimensions takes the form:

$$H : \mathbb{C}^N \otimes \ell^2(\mathbb{Z}^d) \rightarrow \mathbb{C}^N \otimes \ell^2(\mathbb{Z}^d), \quad H = \sum_{y \in \mathbb{Z}^d} W_y \otimes S^y, \quad (2.1)$$

where  $S^y$  is the shift operator by  $y$  on  $\ell^2(\mathbb{Z}^d)$  given by  $S^y|x\rangle = |x+y\rangle$ , and the  $N \times N$  matrices  $W_y$ , called tunneling or hopping matrices, satisfy only the constraint

$$W_y^* = W_{-y},$$

ensuring that  $H$  is self-adjoint. Throughout, we denote the space of  $N \times N$  matrices with complex entries by  $M_N(\mathbb{C})$ . Also,  $\text{tr}$  will denote the trace of matrices, such as those from  $M_N(\mathbb{C})$ , or more general the trace over finite dimensional Hilbert spaces. The trace over infinite Hilbert spaces, such as  $\ell^2(\mathbb{Z}^d)$  or  $\mathbb{C}^N \otimes \ell^2(\mathbb{Z}^d)$ , will be denoted as usual by  $\text{Tr}$ .

The dimension  $N$  of the fiber is determined by the number of molecular orbitals per unit cell of the material included in the model, and the larger this number the more precise the model is. Let us make it clear from the beginning that (2.1) are not toy models, but rather the *models of choice* in materials science. Given a concrete material, such lattice Hamiltonians can be generated empirically by fitting available experimental data or using first-principle calculations [132, 150, 221, 230]. The main tool for generating lattice models from first principles continuous model calculations is the maximally localized Wannier basis set. The reader can find in [136] impressive demonstrations of how effective and accurate this tool can be. Even when working empirically, the lattice models can be finely tuned to accurately reproduce a broad range of experiments and, once such fine tuning is achieved, the models can be used for predictions. An example of this sort is the discovery of the first topological insulator [26]. The *quantitative* predictions based on a lattice model made in [26] were later shown to be extremely accurate by the experiment [121].

Typically, the hopping matrices  $W_y$  in (2.1) decay rapidly with  $y$  and in practice the summation over  $y$  is restricted to a finite number  $\mathcal{R} \subset \mathbb{Z}^d$  of terms, and this will be done from now on. We refer to such Hamiltonians as having finite hopping range. If adequate conditions are imposed on the fall-off of  $W_y$  in  $y$ , the case  $\mathcal{R} = \mathbb{Z}^d$  can be also managed with some further technical effort, but it will not be pursued here. For the periodic models, one can use the Bloch-Floquet decomposition

$$\mathcal{FH}\mathcal{F}^* = \int_{\mathbb{T}^d}^{\oplus} dk H_k \quad (2.2)$$

over the Brillouin torus  $\mathbb{T}^d$ , to reduce the analysis to that of a smooth family of  $N \times N$  matrices

$$H_k : \mathbb{C}^N \rightarrow \mathbb{C}^N, \quad H_k = \sum_{y \in \mathcal{R}} e^{i\langle y|k \rangle} W_y.$$

Throughout,  $\langle \cdot, \cdot \rangle$  will denote the Euclidean scalar product. Examining the classification table, we see that the topological phases in the unitary class are conjectured to occur only in even space dimensions, and for each such dimension there is an infinite sequence of topological phases. It is also conjectured that these phases can be distinguished from one another by tagging them with just one integer number. In the bulk, this number is given by the top even Chern number, which is a measurable physical coefficient (see Chap. 7) and takes the form [13]

$$\text{Ch}_d(P_F) = \frac{(2\pi i)^{\frac{d}{2}}}{(\frac{d}{2})!} \sum_{\rho \in \mathcal{S}_d} (-1)^\rho \int_{\mathbb{T}^d} \frac{dk}{(2\pi)^d} \text{tr} \left( P_F(k) \prod_{j=1}^d \frac{\partial P_F(k)}{\partial k_{\rho_j}} \right), \quad (2.3)$$

for the periodic crystals. Throughout,  $\mathcal{S}_d$  will denote the group of permutations and  $i = \sqrt{-1}$ . In (2.3),

$$P_F(k) = \chi(H_k \leq \mu)$$

is the spectral projection onto the energy bands below the Fermi level  $\mu$ . The standard terminology for it is the Fermi projection. Because we are dealing with insulators, the Fermi level is assumed to be located in a spectral gap of  $H$ . Throughout,  $\chi(A)$  will denote the characteristic function of a set  $A$ . We will present an explicit topological model shortly, but let us mention at this point that the periodic models with  $\text{Ch}_d(P_F) \neq 0$  are ubiquitous. For example, if one generates the hopping matrices  $W_y$  randomly, assuming  $\mathcal{R}$  and  $N$  large, then the chances of obtaining a topological system are far greater than the chances of obtaining a trivial one.

Our analysis, while limited to lattice models, will include uniform magnetic fields and disorder. The presence of a uniform magnetic field is incorporated in the lattice models using the Peierls substitution [157], which amounts to replacing the ordinary shift operators with the dual magnetic translations

$$\mathbf{1} \otimes S^y \mapsto U_{\text{sym}}^y = \mathbf{1} \otimes e^{\frac{i}{2} \langle y | \mathbf{B} | X \rangle} S^y = \mathbf{1} \otimes S^y e^{\frac{i}{2} \langle y | \mathbf{B} | X \rangle}. \quad (2.4)$$

Here,  $\mathbf{B}$  is a real anti-symmetric  $d \times d$  matrix representing the magnetic field and  $X$  is the position operator on  $\ell^2(\mathbb{Z}^d)$ . The label “sym” indicates that the so-called symmetric gauge has been used above. After the substitution, the lattice Hamiltonians take the form

$$H_{\text{sym}} = \sum_{y \in \mathcal{R}} W_y \otimes U_{\text{sym}}^y = \sum_{y \in \mathcal{R}} \sum_{x \in \mathbb{Z}^d} e^{\frac{i}{2} \langle y | \mathbf{B} | x \rangle} W_y \otimes |x\rangle \langle x - y|. \quad (2.5)$$

The Hamiltonian (2.5) is no longer invariant to the ordinary lattice translations. Nevertheless,  $H_{\text{sym}}$  is invariant relative to the magnetic translations

$$V_{\text{sym}}^x H_{\text{sym}} (V_{\text{sym}}^x)^* = H_{\text{sym}}, \quad V_{\text{sym}}^x = \mathbf{1} \otimes e^{-\frac{i}{2} \langle x | \mathbf{B} | X \rangle} S^x = \mathbf{1} \otimes S^x e^{-\frac{i}{2} \langle x | \mathbf{B} | X \rangle}, \quad (2.6)$$

written here also in the symmetric gauge.

A Landau gauge can be defined so that no Peierls phase is generated when the lattice is shifted in the  $d$ -th direction. While the symmetric gauge is more convenient for the bulk analysis, the Landau gauge is obviously more convenient for systems with a boundary in the  $d$ -th direction. The dual and the direct magnetic translations in the Landau gauge can be obtained from the symmetric ones via the transformations

$$U^y = e^{-\frac{i}{2} \langle y | \mathbf{B}_+ | y \rangle} e^{\frac{i}{2} \langle X | \mathbf{B}_+ | X \rangle} U_{\text{sym}}^y e^{-\frac{i}{2} \langle X | \mathbf{B}_+ | X \rangle} = S^y e^{i \langle y | \mathbf{B}_+ | X \rangle} \quad (2.7)$$

and

$$V^x = e^{\frac{i}{2} \langle x | \mathbf{B}_+ | x \rangle} e^{\frac{i}{2} \langle X | \mathbf{B}_+ | X \rangle} V_{\text{sym}}^x e^{-\frac{i}{2} \langle X | \mathbf{B}_+ | X \rangle} = e^{i \langle X | \mathbf{B}_+ | x \rangle} S^x, \quad (2.8)$$

where  $\mathbf{B}_+$  is the lower triangular part of  $\mathbf{B}$ . Note that, indeed, if  $x$  and  $y$  are strictly along the  $d$ -th direction, both  $U^y$  and  $V^x$  reduce to ordinary shifts. By the conjugation of (2.5) with the local unitary operator  $e^{\frac{i}{2}\langle X|\mathbf{B}_+|X\rangle}$  (namely, by a gauge transformation), the Hamiltonian becomes

$$H = e^{\frac{i}{2}\langle X|\mathbf{B}_+|X\rangle} H_{\text{sym}} e^{-\frac{i}{2}\langle X|\mathbf{B}_+|X\rangle} = \sum_{y \in \mathcal{R}} e^{\frac{i}{2}\langle y|\mathbf{B}_+|y\rangle} W_y \otimes U^y. \quad (2.9)$$

It is unitarily equivalent to (2.5) and satisfies  $V^x H (V^x)^* = H$ . As a consequence,  $H$  in (2.9) is periodic in the  $d$ -th direction. We will refer to (2.9) as the representation of the Hamiltonian in the Landau gauge.

A homogeneous disorder will be described by a dynamical system  $(\Omega, \tau, \mathbb{Z}^d, \mathbb{P})$ . Here,  $\Omega$  is a compact metrizable topological space representing the disorder configuration space and  $\tau$  is a homeomorphic action of  $\mathbb{Z}^d$  on  $\Omega$ , describing the behavior of the disorder configurations under the lattice translations. Furthermore  $\mathbb{P}$  is an invariant and ergodic probability measure on  $\Omega$  w.r.t.  $\tau$ , which defines the disorder averaging procedure. A more detailed description of the space of disorder configurations is given in Sect. 2.4.1. If disorder is present, all the coefficients in the Hamiltonian develop a random component and its generic form becomes

$$\begin{aligned} H_{\text{sym}, \omega} &= \sum_{y \in \mathcal{R}} \sum_{x \in \mathbb{Z}^d} W_y(\tau_x \omega) \otimes |x\rangle \langle x| U_{\text{sym}}^y \\ &= \sum_{y \in \mathcal{R}} \sum_{x \in \mathbb{Z}^d} e^{\frac{i}{2}\langle y|\mathbf{B}|x\rangle} W_y(\tau_x \omega) \otimes |x\rangle \langle x - y|, \end{aligned} \quad (2.10)$$

in the symmetric gauge. The hopping matrices  $W_y$  are now continuous functions over  $\Omega$  with values in  $M_N(\mathbb{C})$ . The models with disorder are no longer invariant to the magnetic translations, but this property is replaced by the following covariance relation:

$$V_{\text{sym}}^x H_{\text{sym}, \omega} (V_{\text{sym}}^x)^* = H_{\text{sym}, \tau_x \omega}, \quad x \in \mathbb{Z}^d. \quad (2.11)$$

The Landau representation is obtained by conjugating (2.10) by  $e^{\frac{i}{2}\langle X|\mathbf{B}_+|X\rangle}$ , which gives

$$H_\omega = \sum_{y \in \mathcal{R}} \sum_{x \in \mathbb{Z}^d} e^{\frac{i}{2}\langle y|\mathbf{B}_+|y\rangle} W_y(\tau_x \omega) \otimes |x\rangle \langle x| U^y, \quad (2.12)$$

and the covariance relation becomes

$$V^x H_\omega (V^x)^* = H_{\tau_x \omega}, \quad x \in \mathbb{Z}^d. \quad (2.13)$$

The bulk-boundary analysis will be carried in the Landau gauge, hence we will primarily work with the Hamiltonian (2.12).

Since the origin of the lattice is completely arbitrary and will change every time a crystal is put down and picked up again in the lab, the model of the disordered crystal must include the whole family of covariant Hamiltonians  $H = \{H_\omega\}_{\omega \in \Omega}$ . The notation is appropriate because in the absence of disorder, the entire family consists of just one element, the  $H$  itself. Systems with the covariance property (2.13) are called homogeneous and have remarkable properties. As we shall see later, there exists a Fourier calculus for them which can be used to define a (non-commutative) differential calculus. Also, any such covariant family  $F = \{F_\omega\}_{\omega \in \Omega}$  possesses the self-averaging property that for  $\mathbb{P}$ -almost every configuration  $\omega$  one has

$$\lim_{V \rightarrow \infty} \frac{1}{|V|} \text{Tr}(\Pi_V F_\omega \Pi_V^*) = \int_{\Omega} \mathbb{P}(d\omega') \text{tr}(\Pi_0 F_{\omega'} \Pi_0^*), \quad (2.14)$$

where  $\Pi_V : \mathbb{C}^N \otimes \ell^2(\mathbb{Z}^d) \rightarrow \mathbb{C}^N \otimes \ell^2(V \cap \mathbb{Z}^d)$  is a partial isometry onto the quantum states  $|\alpha\rangle \otimes |x\rangle$  with  $x$  located inside  $V$ . In particular,  $\Pi_0$  is the partial isometry onto the quantum states  $|\alpha\rangle \otimes |0\rangle$ . Identity (2.14) follows directly from Birkhoff's ergodic theorem [27]. The quantity on the l.h.s. of (2.14) is called the trace per volume of the covariant observable  $F$ . It is hence, with probability one, independent of the disorder configuration and is equal to the disorder average of the trace of its matrix elements computed at the origin (or any other point of the lattice). In the following we will use the notation  $\mathcal{T}(F)$  for the trace per volume of a family covariant observables. The top even Chern number can be formulated for the generic models (2.10) or (2.12) using a real-space representation and the trace per volume [169]

$$\text{Ch}_d(P_F) = \frac{(2\pi i)^{\frac{d}{2}}}{\frac{d!}{2!}} \sum_{\rho \in \mathbb{S}_d} (-1)^\rho \mathcal{T}\left(P_\omega \prod_{i=1}^d (i[P_\omega, X_{\rho_i}])\right). \quad (2.15)$$

Here,

$$P_F = \{P_\omega\}_{\omega \in \Omega} = \{\chi(H_\omega \leq \mu)\}_{\omega \in \Omega}$$

is the covariant family of spectral projections onto the energy spectrum below  $\mu$ , that is, the family of Fermi projections. The top even Chern number, as defined in (2.15), is known to remain quantized, non-fluctuating from one disorder configuration to another, and be homotopically stable as long as the Fermi level resides in a region of Anderson-localized spectrum [20, 169]. These statements will be re-examined in Chap. 6.

To model a boundary, the physical space and the models are restricted to the half-space  $\mathbb{Z}^{d-1} \times \mathbb{N}$ . The half-space Hamiltonian  $\hat{H}$  then acts on the Hilbert space  $\mathbb{C}^N \otimes \ell^2(\mathbb{Z}^{d-1} \times \mathbb{N})$ . For the moment being, it can just be thought of as the restriction of  $H$  which corresponds to Dirichlet boundary conditions. In Sect. 2.4.3 other allowed boundary conditions will be described. When the bulk Chern number  $\text{Ch}_d$  does not vanish, the energy spectrum of the half-space Hamiltonian  $\hat{H}$  extends inside the bulk insulating gap, covering it completely [58, 172]. The electron states corre-



sponding to the spectrum inside the bulk insulating gap are exponentially localized near the boundary, hence the terminology boundary states and boundary spectrum (see Sect. 2.4.3 for an explicit example). For periodic crystals with a planar boundary, say  $x_d \geq 0$ , the spectrum can be represented as energy bands rendered as functions of the momentum  $k \in \mathbb{T}^{d-1}$  parallel to the boundary. The hallmark feature of the topological phases from the unitary class is the existence of boundary energy bands that connect the bulk valence and conduction bands. For  $d > 2$ , the boundary bands display one or more singularities called Weyl points. Around a Weyl point, denoted by  $k^W \in \mathbb{T}^{d-1}$  in the following, the spectrum and the states are well described by a Weyl operator

$$\sum_{j=1}^{d-1} v_j (k_j - k_j^W) \sigma_j, \quad (2.16)$$

where  $\sigma = (\sigma_1, \dots, \sigma_{d-1})$  are the generators of an irreducible representation of the odd complex Clifford algebra  $Cl_{d-1}$  and  $v = (v_1, \dots, v_{d-1})$  are the non-vanishing slopes of the bands in different directions parallel to the boundary, which can be positive or negative.

*Remark 2.2.1* In the literature, the singular points (2.16) are sometimes also called Dirac points, which is not appropriate for the following reasons. In 4 dimensions, for example, the zero mass Dirac operator takes the form  $\langle k, \gamma \rangle$  and has a chiral symmetry w.r.t. the product  $\gamma_1 \cdots \gamma_d$ . This splits it into two chiral sectors and, in each of those chiral sectors, one gets the classical Weyl operator  $\langle k, \sigma \rangle$  when the “time” direction is separated out. Here,  $\gamma$  and  $\sigma$  denote the Dirac and Pauli matrices. This pattern can be recognized in any dimension, and in general, the Weyl operator involves an odd number of Clifford generators and does not have a chiral symmetry, but rather a chirality that will be introduced below. Throughout, we will be consistent and use the notation  $\sigma$  ( $\gamma$ ) for the generators of the odd (even) complex Clifford algebras, and refer to the operators  $\langle k, \sigma \rangle$  ( $\langle k, \gamma \rangle$ ) as Weyl (Dirac) operators when the dimension of  $k$  is odd (even), respectively.  $\diamond$

Now, suppose that all the Weyl singularities have been identified from the boundary band spectrum and that the asymptote (2.16) of the Hamiltonian has been extracted for each singularity (dimension  $d = 2$  is special in this respect, see below). Then the chirality of a Weyl point

$$v_W = \prod_{j=1}^{d-1} \text{sgn}(v_j) \in \{-1, 1\}, \quad (2.17)$$

is a well defined topological invariant, provided the Weyl point remains separated from the rest. The central conjectures for the unitary class is the following bulk-boundary principle [172]

$$\text{Ch}_d(P_F) = \chi \sum v_W, \quad (2.18)$$

where the sum on the left goes over all Weyl points. In other words, under deformations of the model, the Weyl singularities will move and possibly collide and annihilate, yet the sum of their chiralities remains the same and equal to the bulk invariant. Above,  $\chi$  is a sign factor which depends on the normalization (or the sign convention) of the bulk invariant and on the specific representation  $\sigma$  of the odd  $d - 1$  dimensional Clifford algebra (recall that there are two inequivalent representations).

In dimension  $d = 2$ , the chiralities are given by the signs of the slopes of the boundary bands traversing the bulk insulating gap. The slopes are computed at a fixed (but arbitrarily chosen) energy level. If a slope of a band happens to be zero, then this band is excluded. The bulk-boundary principle (2.18) was first demonstrated by Hatsugai [87] for the special case of the Harper operator with rational magnetic field. In higher dimension, the bulk-boundary principle will be exemplified on an exactly solvable model in Sect. 2.2.4. A proof of (2.18) will be given in Sect. 5.5, combined with the evaluation of the boundary invariants for periodic systems in Sect. 5.3.

One of the main goals of the present work is to formulate  $\sum \nu_W$  as a boundary topological invariant which makes sense in the presence of disorder and magnetic fields, and to derive an index theorem for it. In dimension  $d = 2$ , this was achieved in [107] and will be reviewed and expanded in Chap. 7. The boundary invariant and the bulk-boundary equation takes the form

$$2\pi \tilde{\mathcal{T}}(J_{\parallel} \rho(\hat{H})) = \text{Ch}_2(P_F) , \quad (2.19)$$

where  $\tilde{\mathcal{T}}$  is the trace per length, taken in the direction parallel with the boundary,  $J_{\parallel}$  is the current operator along the boundary and  $\rho$  is a distribution which integrates to one and has support inside the bulk insulating gap, but is otherwise arbitrary. As above, the Hamiltonian  $\hat{H}$  describes the system with a boundary. Physically, the invariant on the l.h.s. of (2.19) gives the charge current spontaneously carried by the boundary states when they are populated with the distribution  $\rho$ . If the bulk invariant  $\text{Ch}_2(P_F)$  is nonzero, (2.19) automatically ensures that the boundary spectrum cannot display gaps or be localized by disorder. This statement will be generalized to higher dimensions in this work.

## 2.2.2 Experimental Achievements

The prototypical example of a topological condensed matter system from the unitary class is the two-dimensional electron gas subjected to a perpendicular uniform magnetic field for which the integer quantum Hall effect (IQHE) is observed [117]. In this case, the Chern number  $\text{Ch}(P_F)$  equals the Hall conductance of the system and all the characteristics described above have been mapped experimentally with amazing precision. We have been careful not to use the word “material” because this topological state of matter is stabilized by a magnetic field which needs to be externally

maintained. It was Haldane [80] who first realized that two-dimensional materials can display characteristics similar to IQHE without the need of an external magnetic field. The minimal yet not sufficient requirements for this to happen is a unit cell containing two (chemically active) molecular orbitals and complex tunneling matrices between these molecular orbitals. The decisive step towards the experimental realization of a topological material from the unitary class were taken in 2013 in the series of works [40, 41] where a thin film of  $(\text{Bi,Sb})_2\text{Te}_3$ , which in the pristine bulk phase is a time-reversal symmetric topological insulator, was doped with chromium magnetic atoms to induce a gapped ferromagnetic ground state. In the short period since then, there have been quite a number of experimental refinements [16, 44, 95, 97, 125, 126], notably the achievement of the quantum critical regime at the transition between the presumed topological and trivial phases [42]. The scaling analysis with the temperature revealed the existence of the critical point and confirmed beyond any doubt that a new topological state of matter was indeed achieved (see also [227] for numerical simulations and discussion). Other materials [131] and experimental paths have been explored. For example, a topologically non-trivial state was realized in a system of one-dimensional array of optical guides which implemented literally the one-dimensional Aubry-Andre model [127, 212]. The condensed matter system proposed by Haldane [80], in its exact form, was finally realized experimentally with ultra-cold fermions in a periodically modulated optical honeycomb lattice [96]. Here the complex tunneling matrices were tuned using time-modulated pulses. Strong two-dimensional topological insulators were also theoretically predicted [81, 175] and then realized in photonic crystals [215]. Furthermore, they were also theoretically predicted [170, 218, 219, 224] and then realized in phonon or acoustic crystals [144]. Lastly, we should mention that driving a condensed matter systems with time-periodic potentials [116, 133, 177] or by considering incommensurate potentials [128, 167] opens the possibility of experimental realizations of topological states which mimic topological insulators in space dimensions higher than three. Such a system will be discussed in details in Sect. 7.5.

### 2.2.3 Conventions on Clifford Representations

To give a firm meaning to the invariants and also to the index theorems presented in Chap. 6, the following conventions will be adopted throughout.

**Conventions on the Clifford representations (CCR).** Since only the complex classes of topological insulators are investigated, we will only be dealing with the complex Clifford algebras  $Cl_n$ . They are defined by  $n$  generators obeying the commutation relations

$$v_i v_j + v_j v_i = 2 \delta_{ij} \mathbf{1}, \quad v_i^* = v_i, \quad i, j = 1, \dots, n. \quad (2.20)$$

As previously mentioned, when the parity of  $n$  is important, we will use for the generators the symbols  $\sigma$  ( $n$  odd) and  $\gamma$  ( $n$  even) but, if the parity is not important and the discussion can be carried in parallel for the two cases, then we will use the symbol  $v$ . The commutation relations (2.20) are invariant to the operations

$$v'_i = uv_iu^{-1}, \quad v'_i = \sum_j A_{i,j}v_j, \quad (2.21)$$

and their combinations, where  $u$  is any unitary element from the Clifford algebra and  $A$  is an orthogonal matrix form  $M_{n \times n}(\mathbb{R})$ , that is  $AA^T = A^TA = \mathbf{1}$ . Below, we list our conventions.

- (i) The orientation of the physical space is fixed once and for all. In other words, one is allowed to redefine the space directions using only proper orthogonal transformations. For example, the reflections are excluded.
- (ii) The orientation of the generators  $v_i$  is also fixed once and for all. This means that all systems of generators can be connected to a reference one using the transformations in (2.21) with  $A$  a proper orthogonal matrix.
- (iii) Once the previous convention is adopted, we can unambiguously define a chiral element (up to a harmless unitary conjugation), for which we adopt the following normalization

$$v_0 = (-i)^{\lfloor \frac{n}{2} \rfloor} v_1 v_2 \cdots v_n, \quad v_0^* = v_0, \quad v_0^2 = \mathbf{1}.$$

- (iv) For  $n = 2k + 1$ , the commutation relations accept two inequivalent irreducible representations on  $\mathbb{C}^{2^k}$ . In this odd case, the chiral element commutes with the entire  $Cl_{2k+1}$ , hence in an irreducible representation it will be sent to a matrix proportional to unity. Our convention is that  $v_0$  is sent exactly into the identity. In other words, our odd representations are uniquely defined (up to proper isomorphisms) by the previous conventions and by

$$\sigma_1 \sigma_2 \cdots \sigma_{2k+1} = i^k \mathbf{1}. \quad (2.22)$$

For example, the Pauli matrices obey this convention.

- (v) For  $n = 2k$ , the commutation relations accept a unique irreducible representations on  $\mathbb{C}^{2^k}$ . In this case, the chiral element anti-commutes with the generators, hence it provides a grading, which we spell again below

$$\gamma_0 = (-i)^k \gamma_1 \gamma_2 \cdots \gamma_{2k}, \quad \gamma_0^* = \gamma_0, \quad \gamma_0^2 = \mathbf{1}. \quad (2.23)$$

*Example 2.2.2* A well-known particular sequence of irreducible representations can be constructed inductively, starting from the one dimensional representation of  $Cl_1$  given by  $\sigma_1 = 1$ . Then, for  $Cl_2$ ,

$$\gamma_1 = \begin{pmatrix} 0 & 1 \\ 1 & 0 \end{pmatrix}, \quad \gamma_2 = \begin{pmatrix} 0 & -i \\ i & 0 \end{pmatrix}, \quad \gamma_0 = \begin{pmatrix} 1 & 0 \\ 0 & -1 \end{pmatrix},$$

and then one can continue iteratively by building the representation of  $Cl_{2k+1}$  from the one of  $Cl_{2k}$  via

$$\sigma_i = \gamma_i \text{ for } i \leq 2k, \quad \sigma_{2k+1} = \gamma_0,$$

and the representation of  $Cl_{2k+2}$  from the one of  $Cl_{2k+1}$  by

$$\gamma_i = \begin{pmatrix} 0 & \sigma_i \\ \sigma_i & 0 \end{pmatrix} \text{ for } i \leq 2k+1, \quad \gamma_{2k+2} = i \begin{pmatrix} 0 & -1 \\ 1 & 0 \end{pmatrix}, \quad \gamma_0 = \begin{pmatrix} 1 & 0 \\ 0 & -1 \end{pmatrix}.$$

These representations satisfy the normalizations (2.22) and (2.23).  $\diamond$

### 2.2.4 Bulk-Boundary Correspondence in a Periodic Unitary Model

We present here a simple model from the unitary class in even dimension  $d$  which displays a rich phase diagram and yet can be explicitly solved in the bulk and with a boundary. Consider the irreducible representation of  $Cl_d$  from Example 2.2.2 and let  $e_j$  be the generators of  $\mathbb{Z}^d$  and  $S_j$  the associated shifts on  $\ell^2(\mathbb{Z}^d)$ . The Hilbert space of the model is  $\mathbb{C}^{2^{\frac{d}{2}}} \otimes \ell^2(\mathbb{Z}^d)$  and the bulk Hamiltonian is translation invariant and takes the form

$$H = \frac{1}{2i} \sum_{j=1}^d \gamma_j \otimes (S_j - S_j^*) + \gamma_0 \otimes \left( m + \frac{1}{2} \sum_{j=1}^d (S_j + S_j^*) \right). \quad (2.24)$$

The Fermi level is assumed at  $\mu = 0$ . The Bloch-Floquet decomposition gives

$$H_k = \sum_{j=1}^d \gamma_j \sin(k_j) + \gamma_0 \left( m + \sum_{j=1}^d \cos(k_j) \right).$$

As  $(H_k)^2$  is proportional to the identity, there are just two eigenvalues of  $H_k$

$$E_k^\pm = \pm \sqrt{\sum_{j=1}^d \sin^2(k_j) + \left( m + \sum_{j=1}^d \cos(k_j) \right)^2}, \quad (2.25)$$

hence the model displays two  $\frac{d}{2}$ -fold degenerate energy bands, arranged symmetrically relative to  $E = 0$ . There is a spectral gap at the Fermi level, except when  $m = 0$ ,

$\pm 2, \dots, \pm d$ . These are precisely the points where the topological transitions take place. Due to the simplicity of the spectrum, the Fermi projector can be computed explicitly

$$P_k = (E_k^+ - E_k^-)^{-1}(E_k^+ - H_k),$$

and the top even Chern number can be evaluated using Eq. (2.3). An analytical calculation is feasible by counting its jumps at the critical values of  $m$  where the bulk gap closes. This analysis has been carried out in [74], see also [172], and is sketched in the following. At the critical values, the band spectrum displays a set of Dirac singularities.

*Remark 2.2.3* Since the discussion is now about the bulk Hamiltonian, therefore in even  $d$  space dimensions, near the singular points the Hamiltonian takes the form of a Dirac operator rather than a Weyl operator. Hence, the appropriate terminology here is Dirac points rather than Weyl points.  $\diamond$

Both the critical  $m$  values and the location of the Dirac points can be derived from (2.25) by imposing the gap closing condition

$$\sum_{j=1}^d \sin^2(k_j) = 0 \quad \text{and} \quad m + \sum_{j=1}^d \cos(k_j) = 0.$$

These equations have the following solutions:

$$\begin{aligned} m_c^0 &= -d, & k^D &= (0, 0, \dots, 0), \\ m_c^1 &= -d + 2, & k^D &= (\pi, 0, 0, \dots, 0) \text{ plus } \binom{d}{1} \text{ permutations}, \\ m_c^2 &= -d + 4, & k^D &= (\pi, \pi, 0, \dots, 0) \text{ plus } \binom{d}{2} \text{ permutations}, \\ &\vdots \\ m_c^{d-1} &= d - 2, & k^D &= (\pi, \dots, \pi, 0) \text{ plus } \binom{d}{d-1} \text{ permutations}, \\ m_c^d &= d, & k^D &= (\pi, \dots, \pi). \end{aligned}$$

The jumps of the Chern number at the gap closings can be explicitly evaluated [74, 172], allowing us to ultimately compute the actual Chern numbers. Indeed, when the gap is closed, there will be a number of Dirac singularities in the band spectrum, and the jumps of the bulk invariant result entirely from these Dirac points. When the bulk gap is nearly closed, i.e.  $m = m_c + \varepsilon$ ,  $|\varepsilon| \ll 1$ , and near such Dirac singularity, the Bloch Hamiltonian takes an asymptotic form,

$$H_k = \sum_{j=1}^d \alpha_j^D (k - k^D)_j \gamma_j + \varepsilon \gamma_0 + \mathcal{O}(k^2),$$

where  $\alpha_j^D = \pm 1$  if  $k_j^D = 0, \pi$ , respectively. It will convenient to make the change of variables  $\alpha_j^D (k - k^D)_j \rightarrow \xi_j$ , in which case

$$H_k = \langle \xi, \gamma \rangle + \varepsilon \gamma_0 .$$

The contribution to the Fermi projector coming from the band spectrum near the Dirac singularity is

$$P(\xi) = \frac{1}{2} - \frac{1}{2} \frac{\langle \xi, \gamma \rangle + \varepsilon \gamma_0}{\sqrt{\xi^2 + \varepsilon^2}} .$$

To compute the contribution  $\mathcal{J}$  of the band spectrum near  $k^D$  to the total Chern number, we plug  $P(\xi)$  into (2.3)

$$\mathcal{J} = \frac{(2\pi i)^{\frac{d}{2}}}{(\frac{d}{2})!} \frac{-1}{2^{d+1}} \prod_{i=1}^d \alpha_i^D \sum_{\rho \in \mathcal{S}_d} (-1)^\rho \int \frac{dk}{(2\pi)^d} \text{tr} \left( \frac{\varepsilon \gamma_0}{\sqrt{\xi^2 + \varepsilon^2}} \prod_{j=1}^d \frac{\gamma_{\rho_j}}{\sqrt{\xi^2 + \varepsilon^2}} \right) ,$$

where the simplifications are solely due to the properties of the  $\gamma$  matrices. The factor  $\prod_{i=1}^d \alpha_i^D$  represents the Jacobian produced by the change of the variable made above. Up to a factor, the integrand converges to the Dirac-delta distribution, hence the domain of integration can be extended to  $\mathbb{R}^d$ , in which case the integral can be explicitly evaluated and, with our conventions on  $\gamma$ 's, the result is

$$\mathcal{J} = \frac{\chi}{2} \frac{\varepsilon}{|\varepsilon|} \prod_{i=1}^d \alpha_i^D , \quad \chi = (-1)^{\frac{d}{2}+1} .$$

When  $\varepsilon$  is varied from negative to positive values,  $\mathcal{J}$  will jump by twice this quantity, leading to a total jump of  $\chi \sum_D \prod_{i=1}^d \alpha_i^D$  for the bulk invariant, at the gap closing. Here it is assumed that  $m$  increases and the sum is over all Dirac singularities present in the boundary band spectrum. Using the information provided above about the number and locations of the Dirac points, we see that the change of the Chern number at a critical value  $m_c^n$  is

$$\Delta_n \text{Ch}_d(P_F) = \chi (-1)^n \binom{d}{n} .$$

Finally, one can check that  $\text{Ch}_d(P_F) = 0$  for  $m < m_c^0$  by sending  $m$  to  $-\infty$ . Hence for  $m \in (-d + 2n, -d + 2n + 2)$  with  $n = 0, \dots, d-1$ ,

$$\text{Ch}_d(P_F) = \chi \sum_{j=0}^n (-1)^j \binom{d}{j} = \chi (-1)^n \binom{d-1}{n} , \quad (2.26)$$

and  $\text{Ch}_d(P_F) = 0$  for  $m \notin [-d, d]$ .

Let us now consider the case with a boundary. Specifically the Hamiltonian is restricted to the Hilbert space  $\mathbb{C}^{2^{\frac{d}{2}}} \otimes \ell^2(\mathbb{Z}^{d-1} \times \mathbb{N})$  with Dirichlet boundary condition at  $x_d = 0$ . As before, this restriction is denoted  $\widehat{H}$ . The Hamiltonian  $\widehat{H}$  remains

translationally invariant in the first  $d - 1$  direction, hence one can perform a partial Bloch-Floquet decomposition:

$$\mathcal{F}\widehat{H}\mathcal{F}^* = \int_{\mathbb{T}^{d-1}}^{\oplus} dk \widehat{H}_k, \quad \widehat{H}_k : \mathbb{C}^{2^{\frac{d}{2}}} \otimes \ell^2(\mathbb{N}) \rightarrow \mathbb{C}^{2^{\frac{d}{2}}} \otimes \ell^2(\mathbb{N}),$$

with

$$\widehat{H}_k = \sum_{j=1}^{d-1} \sin(k_j) \gamma_j \otimes 1 + \frac{1}{2i} \gamma_d \otimes (\widehat{S} - \widehat{S}^*) + \gamma_0 \otimes \left( m + \sum_{j=1}^{d-1} \cos(k_j) + \frac{1}{2} (\widehat{S} + \widehat{S}^*) \right).$$

Here,  $\widehat{S}$  is the unilateral shift operator on  $\ell^2(\mathbb{N})$ . For  $\widehat{E}_k$  inside the bulk insulating gap, the solutions to the Schrödinger equation  $H_k \psi_k = \widehat{E}_k \psi_k$  must be sought in the form

$$\psi_k(x) = \xi_k \otimes (\lambda_k)^x, \quad |\lambda_k| < 1, \quad \xi_k \in \mathbb{C}^{2^{\frac{d}{2}}}.$$

Writing the Schrödinger equation for generic  $x_d > 0$  and at  $x_d = 0$  with the Dirichlet boundary condition, leads to two independent constraints:

$$\left[ \sum_{j=1}^{d-1} \sin(k_j) \gamma_j + \frac{\lambda_k - \lambda_k^{-1}}{2i} \gamma_d + \left( m + \sum_{j=1}^{d-1} \cos(k_j) + \frac{\lambda_k + \lambda_k^{-1}}{2} \right) \gamma_0 \right] \xi_k = \widehat{E}_k \xi_k,$$

and

$$\left[ \sum_{j=1}^{d-1} \sin(k_j) \gamma_j + \frac{\lambda_k}{2i} \gamma_d + \left( m + \sum_{j=1}^{d-1} \cos(k_j) + \frac{\lambda_k}{2} \right) \gamma_0 \right] \xi_k = \widehat{E}_k \xi_k.$$

Taking the difference of these equation, we obtain the simpler constraints

$$(i\gamma_d + \gamma_0) \xi_k = 0$$

and

$$\left[ \sum_{j=1}^{d-1} \sin(k_j) \gamma_j + \left( m + \sum_{j=1}^{d-1} \cos(k_j) + \lambda_k \right) \gamma_0 \right] \xi_k = \widehat{E}_k \xi_k.$$

It is not difficult to see that these two constraints can be simultaneously satisfied only if the coefficient of  $\gamma_0$  in the last constraint is identically zero. The conclusion is that  $\xi_k \otimes (\lambda_k)^x$  solves the Schrödinger equation with the Dirichlet boundary condition at  $x_d = 0$  if and only if

$$(i\gamma_d + \gamma_0) \xi_k = 0 \quad \text{and} \quad \lambda_k = - \left( m + \sum_{j=1}^{d-1} \cos(k_j) \right).$$



This implies that  $\xi_k$  is a common eigenvector for two commuting matrices:

$$\left[ \sum_{j=1}^{d-1} \sin(k_j) \gamma_j \right] \xi_k = \widehat{E}_k \xi_k ,$$

and

$$-i \gamma_0 \gamma_d \xi_k = -(-i)^{\frac{d}{2}+1} \gamma_1 \cdots \gamma_{d-1} \xi_k = \xi_k . \quad (2.27)$$

For  $d = 2$ , the condition (2.27) is equivalent to  $\gamma_1 \xi_k = \xi_k$ , hence  $\xi_k$  is the unique eigenvector corresponding to the positive eigenvalue of  $\gamma_1$ , denoted by  $\xi_+$  in the following (no dependence on  $k = k_1$ ). The Schrödinger equation  $\widehat{H}_k \psi_k = \widehat{E}_k \psi_k$  then admits a unique solution inside the insulating gap:

$$\widehat{E}_k = \sin(k) , \quad \psi_k(x) = \xi_+ \otimes \frac{(\lambda_k)^x}{\sqrt{2(1 - (\lambda_k)^2)}} , \quad \lambda_k = -(m + \cos(k)) ,$$

which leads to an edge state provided the constraint  $|\lambda_k| < 1$  is satisfied. As one can see, there are no singular points in the boundary band spectrum and  $\widehat{E}_k \approx \pm k$  near  $E = 0$ . The sign depends on where the band crosses the  $E = 0$  mark, which can be at  $k = 0$  or  $\pi$ . The chirality  $v^W$  of the edge band is determined by the constraint  $|\lambda_k| < 1$  which is equivalent to

$$\cos(k) \in [-m - 1, -m + 1] \cap [-1, 1] . \quad (2.28)$$

If  $|m| > 2$ , the constraint (2.28) cannot be fulfilled and consequently there are no edge bands. If  $m \in (-2, 0)$ , then  $k = 0$  does satisfy (2.28), but  $k = \pi$  does not. Hence, the slope of the edge band is positive when it crosses the  $E = 0$  level, hence the chirality  $v^W$  is positive. If  $m \in (0, 2)$ , then  $k = \pi$  does satisfy (2.28), but  $k = 0$  does not. Hence, the slope of the edge band is negative when it crosses the  $E = 0$  level, hence the chirality is negative. These and the values of the Chern number given in (2.26) confirm the bulk-boundary correspondence (2.18) in two space dimensions.

For  $d > 2$ , note that the matrix on the l.h.s. of (2.27) is Hermitean and commutes with all  $\gamma_1, \dots, \gamma_{d-1}$ . Hence, the constraint (2.27) reduces the algebra of  $\gamma_1, \dots, \gamma_{d-1}$  to an irreducible representation of the complex odd Clifford algebra  $Cl_{d-1}$ . Indeed, the dimension of the linear subspace  $\mathcal{L} \subset \mathbb{C}^{\frac{d}{2}}$  spanned by the  $\xi$ 's satisfying (2.27) is  $2^{\frac{d-2}{2}}$ , and this subspace is invariant for the matrices  $\gamma_1, \dots, \gamma_{d-1}$ . Hence we can define the linear operators:

$$\hat{\sigma}_j : \mathcal{L} \rightarrow \mathcal{L} , \quad \hat{\sigma}_j = \gamma_j|_{\mathcal{L}} , \quad j = 1, \dots, d-1 ,$$

which satisfy the Clifford relations  $\hat{\sigma}_i \hat{\sigma}_j + \hat{\sigma}_j \hat{\sigma}_i = 2\delta_{ij}$  for  $i, j = 1, \dots, d-1$ , and the CCR convention  $\hat{\sigma}_1 \cdots \hat{\sigma}_{d-1} = i^{\frac{d-2}{2}} \mathbf{1}_{\mathcal{L}}$ .

We can now draw the conclusions for  $d > 2$ :

- (i)  $\xi_k$ 's are eigenvectors of a reduced Hamiltonian which is a Weyl-type operator

$$\left[ \sum_{j=1}^{d-1} \sin(k_j) \hat{\sigma}_j \right] \xi_k = \widehat{E}_k \xi_k .$$

- (ii) The band spectrum inside the insulating gap is given by

$$\widehat{E}_k^\pm = \pm \sqrt{\sum_{j=1}^{d-1} \sin^2(k_j)} . \quad (2.29)$$

The  $\pm$  branches are connected at a singular point which occurs at  $E = 0$ . This singularity is the Weyl point mentioned earlier. The bands are  $2^{\frac{d-4}{2}}$ -fold degenerate. This degeneracy can be lifted by a small perturbation except at  $E = 0$  where the bands will remain connected via a singularity. It is, however, possible to move the singularity both in  $k$ -space and in energy.

- (iii) The  $2^{\frac{d-4}{2}}$  eigenstates corresponding to  $\widehat{E}_k^\pm$ , respectively, are all of the form

$$\psi_k(x) = \xi_k^\pm \otimes \frac{(\lambda_k)^x}{\sqrt{2(1 - (\lambda_k)^2)}} , \quad \lambda_k = -\left(m + \sum_{j=1}^{d-1} \cos(k_j)\right) .$$

- (iv) Generically, the boundary bands are not defined over the entire Brillouin zone, but only over the domain determined by the implicit condition  $|\lambda_k| < 1$ . By examining (2.25) and (2.29), one can see that if  $k$  is at the edges of this domain, then  $\widehat{E}_k^+$  is aligned with  $\min_{k_d}(E_{k,k_d}^+)$ , and  $\widehat{E}_k^-$  is aligned with  $\max_{k_d}(E_{k,k_d}^-)$ , where  $E_{k,k_d}^\pm$  are the bulk eigenvalues (2.25). These identities are not generic though as it may happen that edge spectrum overlaps bulk spectrum.
- (v) From (2.29), one sees that the coordinates of the Weyl points are restricted to

$$k_j^W \in \{0, \pi\}, \quad j = 1, \dots, d-1 .$$

For  $k$  in a neighborhood of a Weyl point, the reduced Hamiltonian can be approximated by an exact Weyl operator

$$\sum_{j=1}^{d-1} \alpha_j (k_j - k_j^W) \hat{\sigma}_j , \quad (2.30)$$

where the sign factors  $\alpha_j = \pm 1$  are determined by the exact location of the Weyl point in the Brillouin zone. For example, if  $k_j^W = 0$  then  $\sin(k_j) \approx k_j - k_j^W$ , while for  $k_j^W = \pi$  rather  $\sin(k_j) = -(k_j - k_j^W)$ . We recall that the signs of a pair  $(\alpha_i, \alpha_j)$

can always be flipped by a continuous rotation in the  $(k_i, k_j)$  plane. As such, if (2.30) contains an even number of negative  $\alpha_j$ 's, then (2.30) is homotopic with  $+\langle(k - k^W)|\hat{\sigma}\rangle$  and will have a positive chirality. If (2.30) contains an odd number of negative  $\alpha_j$ 's, then (2.30) is homotopic with  $-\langle(k - k^W)|\hat{\sigma}\rangle$  and will have a negative chirality.

- (vi) There can be more than one Weyl point. The condition which determines how many Weyl points are there and where are they exactly located is

$$|\lambda_{k^W}| < 1 \iff \sum_{j=1}^{d-1} \cos(k_j^W) \in [-1 - m, 1 - m] \cap [-d + 1, d - 1] .$$

Now we can demonstrate the bulk-boundary principle (2.18) for this particular model. Indeed, let  $m \in (-d + 2n, -d + 2n + 2)$ . Then there is only one combination (modulo permutations) of  $d - 1$  numbers equal to  $+1$  or  $-1$ , representing the  $\cos(k_j^W)$  appearing in the last equation, such that their sum belongs to the interval  $(-1 - m, 1 - m)$ . Indeed, since

$$(-1 - m, 1 - m) \subset (d - 2n - 1, d - 2n + 1) ,$$

$n$  of these numbers have to be  $-1$  and  $(d - 1 - n)$  of them have to be  $+1$ . There are  $\binom{d-1}{n}$  permutations of these signs, corresponding to as many distinct locations of the Weyl points. Furthermore, precisely  $n$  of the coordinates  $k_j^W$  are equal to  $\pi$  while the remaining are zero, hence the chirality of all Weyl points is the same and equal to  $(-1)^n$ . The conclusion is that the boundary invariant is

$$\sum v_W = (-1)^n \binom{d-1}{n} , \quad m \in (-d + 2n, -d - 2n + 2) ,$$

and hence, when multiplied by the sign factor  $\chi$ , it equals the bulk even Chern number given in (2.26).

## 2.3 The Chiral Unitary Class

The solid state systems from the chiral unitary class have a unitary time evolution semi-group and a sub-lattice symmetry to be described in great length below. Following the same format as for the previous section, we introduce the models and their physical characteristics, both for bulk and for half-space. We formulate the bulk-boundary principle for periodic systems and demonstrate this principle using an exactly solvable model in arbitrary odd dimension. The existing experimental results are briefly surveyed.

### 2.3.1 General Characterization

The lattice models for insulators from the chiral unitary class are defined over the Hilbert space  $\mathbb{C}^{2N} \otimes \ell^2(\mathbb{Z}^d)$ , as the dimension of the fiber is necessarily an even integer. A Hamiltonian  $H$  displays chiral (or sublattice) symmetry if there exists a symmetry  $J$  on  $\mathbb{C}^{2N}$  satisfying  $J^* = J$  and  $J^2 = \mathbf{1}_{2N}$  and having eigenspaces of equal dimension, such that

$$(J \otimes \mathbf{1}) H (J \otimes \mathbf{1}) = -H. \quad (2.31)$$

Throughout, we work with a basis of  $\mathbb{C}^{2N}$  such that  $J$  takes a diagonal form

$$J = \begin{pmatrix} \mathbf{1}_N & 0 \\ 0 & -\mathbf{1}_N \end{pmatrix}, \quad (2.32)$$

We will also write  $J$  instead of  $J \otimes \mathbf{1}$ . The Fermi level is pinned at 0 for the chiral unitary symmetry class which is a point of reflection symmetry of the spectrum of  $H$  by (2.31). Since we deal with insulators, the Fermi level will also be assumed to be in a spectral gap of the bulk Hamiltonian. In this situation the Fermi projection  $P_F = \frac{1}{2}(\mathbf{1} - \text{sgn}(H))$  is given in terms of a unitary  $U_F$  on  $\mathbb{C}^N \otimes \ell^2(\mathbb{Z}^d)$  because (2.31) implies

$$\text{sgn}(H) = \begin{pmatrix} 0 & U_F^* \\ U_F & 0 \end{pmatrix}. \quad (2.33)$$

We will refer to  $U_F$  as the Fermi unitary operator, in analogy with the Fermi projection for the unitary class. It encodes the Fermi projection  $P_F = \chi(H \leq 0)$  of a chiral Hamiltonian via

$$P_F = \frac{1}{2} \begin{pmatrix} \mathbf{1} & -U_F^* \\ -U_F & \mathbf{1} \end{pmatrix}. \quad (2.34)$$

Let us begin by looking at periodic models with vanishing magnetic field. The Hamiltonian  $H : \mathbb{C}^{2N} \otimes \ell^2(\mathbb{Z}^d) \rightarrow \mathbb{C}^{2N} \otimes \ell^2(\mathbb{Z}^d)$  is given by (2.1) together with the chirality constraint, which implies  $W_y = \begin{pmatrix} 0 & w_y \\ w_{-y}^* & 0 \end{pmatrix}$  with  $N \times N$  matrices  $w_y$  so that

$$H = \sum_{y \in \mathbb{Z}^d} \begin{pmatrix} 0 & w_y \\ w_{-y}^* & 0 \end{pmatrix} \otimes S^y. \quad (2.35)$$

Its Bloch-Floquet decomposition (2.2) has fiber Hamiltonians

$$H_k = \sum_{y \in \mathbb{Z}^d} \begin{pmatrix} 0 & e^{i(y|k)} w_y \\ e^{-i(y|k)} w_y^* & 0 \end{pmatrix}.$$

By examining the classification table, we see that the topologically non-trivial phases are conjectured to occur only in odd space dimensions. Furthermore, for each such

dimension, there is an infinite sequence of topological phases and the phases can be distinguished from one another by tagging them with just one integer number. In the bulk, this number is given by the top odd Chern number [190, 193]:

$$\text{Ch}_d(U_F) = \frac{i(\pi)^{\frac{d-1}{2}}}{d!!} \sum_{\rho \in \mathbb{S}_d} (-1)^\rho \int_{\mathbb{T}^d} \frac{dk}{(2\pi)^d} \text{Tr} \left( \prod_{j=1}^d U_F^*(k) \frac{\partial U_F(k)}{\partial k_{\rho_j}} \right), \quad (2.36)$$

where  $U_F(k)$  is the  $N \times N$  matrix appearing in the Bloch-Floquet decomposition  $\mathcal{F}U_F\mathcal{F}^* = \int_{\mathbb{T}^d}^{\oplus} dk U_F(k)$  of the Fermi unitary operator. As we shall see in Chap. 7, the bulk topological invariant for chiral symmetric solid state systems is a physically measurable coefficient.

*Remark 2.3.1* We will use the same notation for the bulk invariants, but it will be always understood that  $\text{Ch}_d$  refers to (2.3) (and its extensions) when  $d$  is even, and to (2.36) (and its extensions) when  $d$  is odd.  $\diamond$

Next, let us write out the generic chiral models with a magnetic field and disorder. In the symmetric gauge, the systems are again described by covariant families of Hamiltonians of the form (2.10), but with the chirality constraint (2.31):

$$\begin{aligned} H_{\text{sym},\omega} &= \sum_{y \in \mathcal{R}} \sum_{x \in \mathbb{Z}^d} \begin{pmatrix} 0 & w_y(\tau_x \omega) \\ w_{-y}(\tau_x \omega)^* & 0 \end{pmatrix} \otimes |x\rangle \langle x| U_{\text{sym}}^y \\ &= \sum_{y \in \mathcal{R}} \sum_{x \in \mathbb{Z}^d} e^{\frac{i}{2} \langle y | \mathbf{B} | x \rangle} \begin{pmatrix} 0 & w_y(\tau_x \omega) \\ w_{-y}(\tau_x \omega)^* & 0 \end{pmatrix} \otimes |x\rangle \langle x - y|. \end{aligned} \quad (2.37)$$

The representation in the Landau gauge, which will be primarily used in the following, is similarly obtained from (2.12):

$$H_\omega = \sum_{y \in \mathcal{R}} \sum_{x \in \mathbb{Z}^d} e^{\frac{i}{2} \langle y | \mathbf{B}_+ | y \rangle} \begin{pmatrix} 0 & w_y(\tau_x \omega) \\ w_{-y}(\tau_x \omega)^* & 0 \end{pmatrix} \otimes |x\rangle \langle x| U^y. \quad (2.38)$$

Here  $w_y$  are continuous functions on the space of disorder configurations  $\Omega$ . The top odd Chern number has a real-space representation [139, 171], which can be applied to models like (2.38). With the notation introduced in the previous section,

$$\text{Ch}_d(U_F) = \frac{i(\pi)^{\frac{d-1}{2}}}{d!!} \sum_{\rho} (-1)^\rho \mathcal{T} \left( \prod_{i=1}^d U_\omega^* i[U_\omega, X_{\rho_i}] \right), \quad (2.39)$$

where  $U_F = \{U_\omega\}_{\omega \in \Omega}$  is the covariant family of Fermi unitary operators. The invariant  $\text{Ch}_d(U_F)$  is known to remained quantized, non-fluctuating from one disorder configuration to another, and be homotopically stable as long as the Fermi level resides in a region of dynamically localized spectrum, see [171] and Chap. 6.

When a chiral symmetry preserving boundary is present and  $\text{Ch}_d(U_F) \neq 0$ , the energy spectrum extends inside the bulk insulating gap. The boundary spectrum does not necessarily cover the entire insulating gap. A situation when this doesn't happen is when a magnetic field perpendicular to the surface of a three-dimensional crystal breaks the boundary spectrum into a Hofstadter pattern. The case  $d = 1$  is special and, since it was already discussed in Chap. 1, it will be excluded from the following discussion. For periodic crystals with a planar boundary, say  $x_d \geq 0$ , and in the absence of magnetic fields, the boundary states can be determined as a function of momentum  $k$  parallel to the boundary. The hallmark feature is the existence of boundary energy bands displaying Dirac singularities at  $E = 0$  [90, 192]. Around a Dirac point  $k^D$ , the spectrum and the states are well described by a Dirac operator

$$\sum_{j=1}^{d-1} v_j (k_j - k_j^D) \gamma_j, \quad (2.40)$$

where  $\gamma$  are the generators of the irreducible representation of the complex even Clifford algebra  $Cl_{d-1}$  (fixed by our conventions) and  $v_j$  are the slopes of the bands at  $E = 0$ . Now a chirality  $v_D = \prod_{j=1}^{d-1} \text{sgn}(v_j)$  can be defined for each Dirac point, just as for the Weyl points in Sect. 2.2. The central conjecture for the chiral unitary class is the following bulk-boundary principle [190]:

$$\text{Ch}_d(U_F) = \chi \sum v_D, \quad (2.41)$$

where the sum carries over all Dirac singularities located at  $E = 0$  of the boundary band spectrum, and  $\chi$  is again a sign which depends on the representations of the Clifford algebras and normalization of the bulk invariant. One conclusion that can be drawn from this principle is that, as long as  $\text{Ch}_d(U_F) \neq 0$ , there will always be boundary bands at  $E = 0$ . Hence, unavoidably, the insulator becomes metallic when a boundary is present. Similarly as for the unitary class, it is one of the main goals of the present work to formulate  $\sum v_D$  as a boundary topological invariant which makes sense in the presence of magnetic fields and disorder, to derive an index theorem for it and to establish (2.41). Among other things, this will enable us to demonstrate that the boundary energy spectrum at  $E = 0$  remains extended in the presence of disorder whenever  $\text{Ch}_d(U_F) \neq 0$ .

We now come to the extremely important point of choosing the unit cell of the crystal. This determines which states are regrouped in the fibers  $\mathbb{C}^{2N}$  and which are the hopping matrices in the Hamiltonian (2.38). It is well-known in the physics community that the value of the bulk invariant for the chiral class depends on this process. We will carry out the discussion on a model in dimension  $d = 1$  which describes a chain with two different atoms (as in [92], p. 22, for example). Figure 2.1 shows two alternating molecular states (or two alternating atoms) and two alternating hopping matrices (the horizontal links). Each of the choices (a), (b) and (c) of the unit cell lead to a different chiral unitary operator  $U_F^{(a)}$ ,  $U_F^{(b)}$  and  $U_F^{(c)}$ , respectively. For

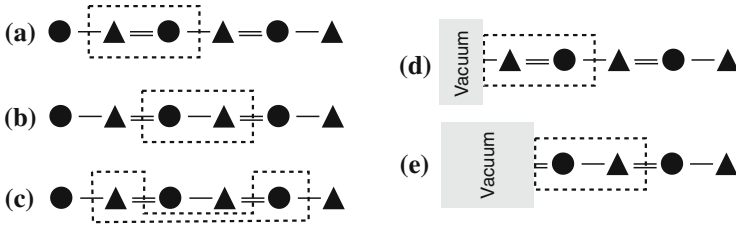


**Fig. 2.1** Graphical representation of the model (1.1) as a molecular chain containing two species of atoms with alternating hopping amplitudes. Panels **a–c** show various possibilities to choose the unit cell. Panels **d–e** show the unique unit cells compatible with the given boundaries

adequate fixed values of the parameters, one finds  $\text{Ch}_d(U_F^{(a)}) = 0$ ,  $\text{Ch}_d(U_F^{(b)}) = 1$  and  $\text{Ch}_d(U_F^{(c)}) = 2$ , respectively. Furthermore, [208] showed that, using certain isomorphisms defined in momentum space, one can change  $\text{Ch}_d$  by any even number. In the real space representation, one such isomorphism corresponds to redefining the unit cell in panel (a) into the unit cell in panel (c). This arbitrariness is very puzzling at first sight for, given a concrete problem, how are we going to predict the physical surface properties from the bulk invariant? The issue has a very simple resolution: The boundary itself dictates which *unique* unit cell is to be used in the computation of the bulk invariant. Thus the rule is that the boundary never cuts through a unit cell, which mathematically means that the fiber subspaces are either erased or kept, entirely, but never split. For example, if the boundary is as in panel (d), then only the unit cell shown in panel (a) obeys this rule, and if the boundary is as in panel (e), then only the unit cell shown in panel (b) obeys the rule. The unit cells of the type shown in panel (c) will always be cut through by a boundary, hence they can be dropped from the beginning. These conclusions apply also in higher space dimensions where one needs  $d$  boundaries to uniquely determine the bulk unit cell and hence the Fermi unitary as well as its Chern number.

### 2.3.2 Experimental Achievements

We should make clear from the start that the chiral symmetry is never exact in solid state systems. After all, the non-relativistic Schrodinger operators are bounded from below and the spectrum extends all the way to  $+\infty$ . The chiral symmetry should be sought in the electron spectrum near the Fermi level, which determines most of the electronic properties of materials. Moreover, it will be shown below that for approximate chiral systems, namely those obtained by a sufficiently small perturbation of an exact chiral system, one can still define a Fermi unitary and its Chern number. Hence non-trivial odd Chern numbers do not require exact chiral symmetry, but in such conditions the delocalized character of the boundary states is lost, in general. There are, however, several materials where chiral symmetry can be

assumed virtually exact. The prototypical examples of strong topological materials from the chiral unitary class are the one-dimensional conducting polymers, with poly-acetylene as the prominent representative [14]. The Su-Schrieffer-Heeger model [205] used in our introductory Chap. 1 was developed precisely for the description of poly-acetylene. The conducting polymers are  $\pi$ -conjugated organic molecular chains which in the absence of lattice distortions would have extended  $\pi$ -molecular orbitals and would display a metallic character. The systems, however, are unstable to Peierls lattice distortions which double the original repeating cells [14]. These distortions open small gaps at the Fermi level and drive these systems into an insulating chiral topological phase. There is a tremendous interest in these materials, not because of their topological properties, but because these polymers can become again metallic when doped with strong oxidizing or reducing agents [43], thus paving the way for conducting plastics [43].

Graphene [148, 149] is a two-dimensional crystal which also displays the chiral symmetry. The band spectrum of graphene is gapped everywhere except at two special points of the Brillouin zone, hence graphene can be considered as a special case of weak topological material from the chiral class. Its honeycomb lattice can be cleaved along the zigzag, the bearded or the arm-chair edges, all of which preserve the chiral symmetry. Using a partial Bloch-Floquet transformation in the momentum  $k$  parallel with the boundary, one obtains families of  $k$ -dependent one-dimensional chiral symmetric Hamiltonians. Excepting two  $k$  values, these Hamiltonians are gapped and hence one can compute the bulk invariant [88]. Whenever the invariant takes a non-trivial value, boundary states occur at  $E = 0$  which ultimately lead to dispersionless boundary bands. It is known that such dispersionless edge states exist along the zigzag edge [72]. The bearded edge is unstable for graphene, but it was engineered in photonic crystals and the dispersionless edge states were confirmed [161]. There are no edge states along the armchair edge. The different behaviors are due to the fact that the unit cell changes from one boundary to another (cf. discussion above). Alternatively, these characteristics of graphene can be explained directly using the boundary invariant [88].

In a recent development, Kane and Lubensky [98] have discovered that, within the harmonic approximation, any isostatic mechanical lattice has a built-in chiral symmetry. They also demonstrated, theoretically, the mechanical analog of the one dimensional Su-Schrieffer-Heeger model and constructed weak chiral symmetric topological mechanical materials in two and three dimensions. These theoretical predictions have recently been confirmed in the lab [155].

So far, we have only mentioned the weak topological insulators in higher dimensions. The search for the strong topological materials with exact (or weakly broken) chiral symmetry is vigorously underway. For example, there are several feasible proposals to realize such systems with cold atoms trapped in optical lattices [216, 217]. Our Sect. 7.4 should be a helpful theoretical contribution to this search.



### 2.3.3 Bulk-Boundary Correspondence in a Periodic Chiral Model

Here we present a simple model from the chiral unitary class which displays a rich phase diagram and yet can be explicitly solved in the bulk and with a boundary. Let  $\gamma$  be the generators of the irreducible representation of  $Cl_{d+1}$  from Example 2.2.2. Using the same notations as in Sect. 2.2.4, the bulk Hamiltonian acting now on  $\mathbb{C}^{2^{\frac{d+1}{2}}} \otimes \ell^2(\mathbb{Z}^d)$  is

$$H = \frac{1}{2i} \sum_{j=1}^d \gamma_j \otimes (S_j - S_j^*) + \gamma_{d+1} \otimes \left( m + \frac{1}{2} \sum_{j=1}^d (S_j + S_j^*) \right).$$

It has the required chiral symmetry  $\gamma_0 H \gamma_0 = -H$ . Its Bloch-Floquet fibers

$$H_k = \sum_{j=1}^d \sin(k_j) \gamma_j + \left( m + \sum_{j=1}^d \cos(k_j) \right) \gamma_{d+1}$$

have just two eigenvalues

$$E_k^\pm = \pm \sqrt{\sum_{j=1}^d \sin^2(k_j) + \left( m + \sum_{j=1}^d \cos(k_j) \right)^2}. \quad (2.42)$$

Hence the model displays two  $\frac{d+1}{2}$ -fold degenerate energy bands arranged, symmetrically relative to  $E = 0$ . There is a spectral gap at  $E = 0$ , except when  $m$  is equal to  $\pm 1, \pm 3, \dots, \pm d$ . These are precisely the points where the topological transitions take place. Due to the simplicity of the spectrum, the Fermi unitary matrix  $U_k$  can be computed explicitly to be

$$U_k = (E_k^+)^{-1} \left[ \sum_{j=1}^d \sin(k_j) \sigma_j + i \left( m + \sum_{j=1}^d \cos(k_j) \right) \mathbf{1} \right],$$

where  $\sigma_j$ 's are the irreducible representation of the odd complex Clifford algebra  $Cl_d$  on  $\mathbb{C}^{2^{\frac{d-1}{2}}}$  (with our CCR conventions). The top odd Chern number can again be computed by counting the change at the critical values of  $m$  where the bulk gap closes, as done for the unitary case. Formally, the gap closing conditions are exactly the same as in the unitary case, and the analysis can be adapted. Near a gap closing, the contribution  $\mathcal{J}$  to the bulk invariant becomes

$$\mathcal{J} = \frac{i(\pi)^{\frac{d-1}{2}}}{d!!} \prod_{i=1}^d \alpha_i^D \sum_{\rho \in \mathbb{S}_d} (-1)^\rho \int \frac{dk}{(2\pi)^d} \text{tr} \left( \frac{-i\varepsilon}{\sqrt{\xi^2 + \varepsilon^2}} \prod_{j=1}^d \frac{\sigma_{\rho_j}}{\sqrt{\xi^2 + \varepsilon^2}} \right),$$

which can be computed explicitly

$$\mathcal{J} = \frac{\chi}{2} \frac{\varepsilon}{|\varepsilon|} \prod_{i=1}^d \alpha_i^W, \quad \chi = (-1)^{\frac{d-1}{2}},$$

where one should note that now we have Weyl singularities at the gap closing. By literally repeating the counting done for the unitary case, we conclude

$$\text{Ch}_d(U_F) = \chi (-1)^n \binom{d-1}{n}, \quad (2.43)$$

for  $m \in (-d+2n, -d+2n+2)$  with  $n = 0, \dots, d-1$ , and  $\text{Ch}_d(U_F) = 0$  otherwise.

We now impose the Dirichlet boundary condition at  $x_d = 0$ . As before, a partial Bloch-Floquet decomposition has fibers

$$\hat{H}_k = \sum_{j=1}^{d-1} \sin(k_j) \gamma_j \otimes 1 + \frac{1}{2i} \gamma_d \otimes (\hat{S} - \hat{S}^*) + \gamma_{d+1} \otimes \left( m + \sum_{j=1}^{d-1} \cos(k_j) + \frac{1}{2} (\hat{S} + \hat{S}^*) \right),$$

and the solutions to the Schrödinger equation  $\hat{H}_k \psi_k = \hat{E}_k \psi_k$  are sought in the form

$$\psi_k(x) = \xi_k \otimes (\lambda_k)^x, \quad |\lambda_k| < 1, \quad \xi_k \in \mathbb{C}^{2^{\frac{d+1}{2}}},$$

Due to the Dirichlet boundary condition at  $x_d = 0$  this leads to the two independent constraints

$$\left[ \sum_{j=1}^{d-1} \sin(k_j) \gamma_j + \frac{\lambda_k - \lambda_k^{-1}}{2i} \gamma_d + \left( m + \sum_{j=1}^{d-1} \cos(k_j) + \frac{\lambda_k + \lambda_k^{-1}}{2} \right) \gamma_{d+1} \right] \xi_k = \hat{E}_k \xi_k,$$

and

$$\left[ \sum_{j=1}^{d-1} \sin(k_j) \gamma_j + \frac{\lambda_k}{2i} \gamma_d + \left( m + \sum_{j=1}^{d-1} \cos(k_j) + \frac{\lambda_k}{2} \right) \gamma_{d+1} \right] \xi_k = \hat{E}_k \xi_k.$$

They can be simultaneously satisfied if only if

$$(i\gamma_d + \gamma_{d+1}) \xi_k = 0 \quad \text{and} \quad \lambda_k = - \left( m + \sum_{j=1}^{d-1} \cos(k_j) \right).$$

This implies that  $\xi_k$  is a common eigenvector for two commuting matrices:

$$\left[ \sum_{j=1}^{d-1} \sin(k_j) \gamma_j \right] \xi_k = \widehat{E}_k \xi_k , \quad (2.44)$$

and

$$-i \gamma_{d+1} \gamma_d \xi_k = \xi_k . \quad (2.45)$$

Let  $\mathcal{L} \subset \mathbb{C}^{2^{\frac{d+1}{2}}}$  be the linear space spanned by the  $\xi$ 's satisfying (2.45) whose dimension is  $2^{\frac{d-1}{2}}$ . This linear space is invariant for the matrices  $\gamma_1, \dots, \gamma_{d-1}$  so that one can define

$$\hat{\gamma}_j = \gamma_j \mid_{\mathcal{L}} , \quad j = 1, \dots, d-1 ,$$

as well as  $\hat{\gamma}_0 = \gamma_0 \mid_{\mathcal{L}} = (-i)^{\frac{d-1}{2}} \hat{\gamma}_1 \cdots \hat{\gamma}_{d-1}$ . This provides an irreducible representation of the even complex Clifford algebra  $Cl_{d-1}$  on  $\mathcal{L}$ , satisfying our conventions. We are now ready to draw our conclusions for  $d > 1$ :

- (i)  $\xi_k$ 's are eigenvectors of a reduced Hamiltonian which is of Dirac-type

$$\left[ \sum_{j=1}^{d-1} \sin(k_j) \hat{\gamma}_j \right] \xi_k = \widehat{E}_k \xi_k .$$

- (ii) The band spectrum inside the insulating gap is given by

$$\widehat{E}_k^{\pm} = \pm \sqrt{\sum_{j=1}^{d-1} \sin^2(k_j)} . \quad (2.46)$$

The  $\pm$  branches are connected at a singular point which occurs at  $E = 0$ . This singularity is the Dirac point mentioned earlier. The bands are  $2^{\frac{d-3}{2}}$ -fold degenerate. This degeneracy can be lifted by a small periodic perturbation except at the Weyl point where the bands will remain connected via a singularity.

- (iii) The  $2^{\frac{d-3}{2}}$  eigenstates corresponding to  $\widehat{E}_k^{\pm}$  are all of the form

$$\psi_k(x) = \xi_k^{\pm} \otimes \frac{(\lambda_k)^x}{\sqrt{2(1 - (\lambda_k)^2)}} , \quad \lambda_k = -\left(m + \sum_{j=1}^{d-1} \cos(k_j)\right) .$$

- (iv) Generically, the boundary bands are not defined over the entire Brillouin zone, but only over the domain determined by the implicit condition  $|\lambda_k| < 1$ .

- (v) From (2.46), the  $d - 1$  coordinates  $k_j^D$  of the Dirac points can only be equal to 0 or  $\pi$ . For  $k$  in a neighborhood of such a Dirac point, the reduced Hamiltonian can be approximated by an exact Dirac operator

$$H_k \approx \sum_{j=1}^{d-1} \alpha_j (k_j - k_j^D) \hat{\gamma}_j, \quad (2.47)$$

where the sign factors  $\alpha_j = \pm 1$  are determined by the exact location of the Dirac point in the Brillouin zone. We can always flip the signs of a pair  $(\alpha_i, \alpha_j)$  by a continuous rotation in the  $(k_i, k_j)$  plane. As such, the Hamiltonians (2.47) fall into two homotopy classes, one of positive chirality for which (2.47) contains an even number of negative  $\alpha_j$ 's, and one of negative chirality for (2.47) which contains an odd number of negative  $\alpha_j$ 's.

- (vi) There could be more than one Dirac point. The condition which determines how many Dirac points are there and where are they exactly located is:

$$|\lambda_k^D| < 1 \iff \sum_{j=1}^{d-1} \cos(k_j^D) \in [-1 - m, 1 - m] \cap [-(d - 1), d - 1].$$

The bulk-boundary correspondence can now be established following line by line the arguments provided for the unitary case.

## 2.4 Main Hypotheses on the Hamiltonians

This section translates the settings and the assumptions in a mathematically precise language and presents the behavior of various quantities of interest under such circumstances. Most of the statements are well-known or can be found in the literature, hence some are presented without a proof. Having all these statements listed in one place will be useful because they are referenced often throughout the book.

### 2.4.1 The Probability Space of Disorder Configurations

Here an explicit mathematical definition of the dynamical system  $(\Omega, \tau, \mathbb{Z}^d, \mathbb{P})$  describing the disorder configurations of the models is given. Throughout it will be assumed that this particular set-up is given. Recall that the allowed hopping range  $\mathcal{R} \subset \mathbb{Z}^d$  is supposed to be finite.

**Definition 2.4.1** Suppose that the randomness in the individual hopping process by  $y \in \mathbb{Z}^d$  can be described by a compact and convex (hence contractible) space  $\Omega_0^y$  equipped with the probability measure  $\mathbb{P}_0^y$ . Then the dynamical system  $(\Omega, \tau, \mathbb{Z}^d, \mathbb{P})$  is defined by:

(i) The compact and metrizable Tychonov space

$$\Omega = \left( \prod_{y \in \mathcal{R}} \Omega_0^y \right)^{\mathbb{Z}^d}. \quad (2.48)$$

(ii) The family of homeomorphisms

$$(\tau_z \omega)_x^y = \omega_{x-z}^y, \quad \omega = \left( \omega_x^y \right)_{x \in \mathbb{Z}^d}^{y \in \mathcal{R}} \in \Omega, \quad z \in \mathbb{Z}^d.$$

In particular, the homeomorphisms corresponding to the generators  $e_j$  of  $\mathbb{Z}^d$  will be denoted by  $\tau_j$ , so that  $\tau_z = \tau_1^{z_1} \dots \tau_d^{z_d}$ .

(iii) The product probability measure

$$\mathbb{P}(d\omega) = \prod_{y \in \mathcal{R}} \prod_{x \in \mathbb{Z}^d} \mathbb{P}_0^y(d\omega_x^y), \quad (2.49)$$

which is invariant and ergodic w.r.t. the  $\mathbb{Z}^d$  action  $\tau$ .

For sake of concreteness, let us give a very concrete and simple example of  $\Omega$  and also the matrix functions  $W_y$  entering into the Hamiltonian (2.12). One may choose  $\Omega_0^y = [-\frac{1}{2}, \frac{1}{2}]$  with  $\mathbb{P}_0(d\omega_x^y) = d\omega_x^y$ , and

$$W_y(\omega) = (1 + \lambda_y \omega_0^y) W_y$$

with real coefficients  $\lambda_y$  which can be seen as a measure of disorder strength.

One last but important observation spurs from the fact that the space  $\Omega$  is contractible. In this case, all the maps are homotopic with the constant map. As a consequence, the map  $\tau$  and the identity map are homotopically equivalent. This will have an important consequence for the K-theory of the observables algebras.

### 2.4.2 The Bulk Hamiltonians

The analysis carried out in this book applies to the families of Hamiltonians  $H = \{H_\omega\}_{\omega \in \Omega}$  defined in (2.12) and (2.38), and indexed by the disorder probability space  $(\Omega, \tau, \mathbb{Z}^d, \mathbb{P})$  described in Definition 2.4.1. These families of Hamiltonians satisfy the covariance relation (2.13). The bulk analysis can be carried out as well in the symmetric gauge but, to avoid confusion, we consider only the Landau gauge from now on. Almost surely, the spectra of  $H_\omega$  are identical non-random sets (see e.g. [49]). This non-random set can be regarded as the spectrum of  $H$ , the family of covariant Hamiltonians.

**Bulk Gap Hypothesis (BGH):** *The Fermi level  $\mu \in \mathbb{R}$  lies in a gap  $\Delta \subset \mathbb{R}$  of the spectrum of  $H$ .*

The gap mentioned above will be referred as the bulk or insulating gap. By a well-known Combes-Thomas estimate (e.g. [53]) one deduces the following estimate on the Fermi projection.

**Proposition 2.4.2** *If BGH holds, then the Fermi projection has exponential decay*

$$\sup_{\omega \in \Omega} |\langle x | \chi(H_\omega \leq \mu) | y \rangle| \leq \gamma e^{-\beta|x-y|}, \quad (2.50)$$

for some strictly positive and finite constants  $\gamma$  and  $\beta$ .

A periodic insulator has, by definition, always a bulk gap. Turning on a disordered perturbation will ultimately close the bulk gap. Nevertheless, it is possible that the Fermi level lies in a region of dynamically Anderson localized spectrum. In this regime, the Fermi level is located in the essential spectrum, but the spectrum is dense pure point and the eigenvectors decay exponentially at infinity. This regime can nicely be characterized by requiring the means square replacement to be bounded [20], however, for sake of simplicity and because it holds in many random models anyway (in particular, those considered here, see [53]), we choose to characterize this regime by the stronger Aizenmann-Molchanov bound [2].

**Mobility Bulk Gap Hypothesis (MBGH):** *The Fermi level  $\mu \in \mathbb{R}$  lies in an interval  $\Delta \subset \mathbb{R}$  of the spectrum of  $H$  which is Anderson localized, in the sense that the Aizenmann-Molchanov bound on the resolvent*

$$\int_{\Omega} \mathbb{P}(d\omega) |\langle x | (E + i\varepsilon - H_\omega)^{-1} | y \rangle|^s \leq \gamma_s e^{-\beta_s|x-y|} \quad (2.51)$$

holds uniformly as  $\varepsilon \rightarrow 0$ , for all  $E \in \Delta$  and any  $s \in (0, 1)$ . Above,  $\gamma_s$  and  $\beta_s$  are strictly positive and finite parameters which depend only on  $s$ .

**Definition 2.4.3** We say that the energy spectrum is delocalized at energy  $E$  if the uniform Aizenmann-Molchannov bound (2.51) cannot be established.

The physical regime where BGH is replaced by MBGH is often referred to as the strong localization regime. The existence of a mobility gap also induces a special behavior on the Fermi projection.

**Proposition 2.4.4** ([1, 53, 169]) *If MBGH holds, then, on average, the Fermi projection is exponentially localized*

$$\int_{\Omega} \mathbb{P}(d\omega) |\langle x | \chi(H_\omega \leq \mu) | y \rangle| \leq \gamma e^{-\beta|x-y|} \quad (2.52)$$

for some strictly positive and finite constants  $\gamma$  and  $\beta$ .

Next we describe the behavior of the Fermi projections under homotopies. To describe the deformations of the covariant Hamiltonians properly, recall that the hopping matrices are continuous functions over  $\Omega$  with values in  $M_N(\mathbb{C})$ . As such, it is natural to view  $W_y$  as elements of the  $C^*$ -algebra  $M_N(\mathbb{C}) \otimes C(\Omega)$ , where  $C(\Omega)$  is equipped with the supremum norm

$$\|\phi\|_{C(\Omega)} = \sup_{\omega \in \Omega} |\phi(\omega)|.$$

**Definition 2.4.5** We call  $t \in [0, 1] \mapsto H(t)$  a continuous deformation of a family of a covariant Hamiltonians  $H$  if  $H(t)$  are covariant families of Hamiltonians obtained by continuous variations of  $W_y$  in  $M_N(\mathbb{C}) \otimes C(\Omega)$ , for every  $y \in \mathbb{R}$ .

Here it is understood that  $\mathcal{R}$  is sufficient large (but finite) to account for all the non-zero hopping matrices during the variation of  $t \in [0, 1]$ . Note that the alignment of the Fermi level with respect to the spectrum can be changed by adding a constant to  $H$ , and this can be done by modifying  $W_0$ . In other words, the above definition of deformations includes also the continuous variations of the Fermi level relative to the spectrum.

**Proposition 2.4.6** *The following holds:*

- (i) *Let  $t \in [0, 1] \mapsto H(t)$  be a continuous deformation such that BGH holds for all  $t$ . Then*

$$\sup_{\omega \in \Omega} \left| \langle x | \chi(H_\omega(t') \leq \mu) - \chi(H_\omega(t) \leq \mu) | y \rangle \right| \leq C(t, t') e^{-\beta|x-y|},$$

*where  $\beta$  is a strictly positive constant (hence independent of  $t$  or  $t'$ ) and  $C(t, t')$  is a continuous function of the arguments, such that  $C(t, t) = 0$  for all  $t \in [0, 1]$ .*

- (ii) *If BGH is replaced by MBGH above, then [181]*

$$\int_{\Omega} \mathbb{P}(d\omega) \left| \langle x | \chi(H_\omega(t') \leq \mu) - \chi(H_\omega(t) \leq \mu) | y \rangle \right| \leq C(t, t') e^{-\beta|x-y|}.$$

The above statements apply to both the unitary and chiral unitary Hamiltonians. The latter class posses a chirality operator, which is a selfadjoint operator  $J : \mathbb{C}^{2N} \otimes \ell^2(\mathbb{Z}^d) \rightarrow \mathbb{C}^{2N} \otimes \ell^2(\mathbb{Z}^d)$ , with  $J = J^*$  and squaring to  $J^2 = \mathbf{1}$  and commuting with the position operator, i.e.  $J$  is local.

**Chirality Hypothesis (CH):** *The family  $H$  of covariant Hamiltonians has an (exact) chiral symmetry if and only if  $JH_\omega J = -H_\omega$  for all  $\omega \in \Omega$ .*

Throughout, we will chose a basis for  $\mathbb{C}^{2N}$  such that the chirality operator is in the diagonal form given in (2.32). Then all chiral symmetric Hamiltonians take the form shown in Eq. (2.38). We recall that the Fermi level is fixed at  $\mu = 0$  for the chiral unitary class.

**Proposition 2.4.7** *Suppose BGH and CH hold. Then:*

(i) The family  $\text{sgn}(H)$  is chiral symmetric and is of the form

$$\text{sgn}(H_\omega) = \begin{pmatrix} 0 & U_\omega^* \\ U_\omega & 0 \end{pmatrix}.$$

(ii) The family  $U_F = \{U_\omega\}_{\omega \in \Omega}$  is covariant and unitary on  $\mathbb{C}^N \otimes \ell^2(\mathbb{Z}^d)$ . In analogy with the Fermi projection,  $U_F$  will be called the Fermi unitary operator.

(iii) The matrix elements of  $U_\omega$  are exponentially localized

$$\sup_{\omega \in \Omega} |\langle x | U_\omega | y \rangle| \leq \gamma e^{-\beta|x-y|},$$

for some strictly positive and finite constants  $\gamma$  and  $\beta$ .

(iv) If BGH is replaced by MBGH, then (i)-(iii) hold with the modification

$$\int_{\Omega} \mathbb{P}(d\omega) |\langle x | U_\omega | y \rangle| \leq \gamma e^{-\beta|x-y|}.$$

*Proof* (i) We have  $\text{sgn}(H) = \mathbf{1}_{2N} - 2P_F$ . Since  $JP_FJ = \mathbf{1}_{2N} - P_F$ , the first part of the statement follows. The second part is a consequence of the chirality. (ii) Because  $U_F$  is obtained by functional calculus from a covariant family of operators, it is itself covariant. Since  $\text{sgn}(H)^2 = \mathbf{1}$ , one has  $U_\omega U_\omega^* = U_\omega^* U_\omega = \mathbf{1}_N$ . The statements (iii) and (iv) follow from Propositions 2.4.2 and 2.4.4 and the formula in (i).  $\square$

When discussing the continuous deformations for models from the chiral unitary class, we use Definition 2.4.5 with the added assumption that, at all times,  $H(t)$  remains chiral symmetric relative to the same  $J$ .

**Proposition 2.4.8** *The following holds:*

(i) Let  $t \in [0, 1] \mapsto H(t)$  be a continuous deformation of  $H$  and assume that BGH and CH hold for all  $t$ . Then

$$\sup_{\omega \in \Omega} |\langle x | U_\omega(t') - U_\omega(t) | y \rangle| \leq C(t, t') e^{-\beta|x-y|},$$

where  $\beta$  is a strictly positive constant (hence independent of  $t$  or  $t'$ ) and  $C(t, t')$  is a continuous function of the arguments, such that  $C(t, t) = 0$  for all  $t \in [0, 1]$ .

(ii) If BGH is replaced by MBGH above, then

$$\int_{\Omega} \mathbb{P}(d\omega) |\langle x | U_\omega(t') - U_\omega(t) | y \rangle| \leq C(t, t') e^{-\beta|x-y|}.$$

*Proof* Both statements follow from Propositions 2.4.6 and 2.4.7.  $\square$

As already pointed out, for the physical materials, the chiral symmetry does not hold exactly but only approximately. In the following we introduce a notion of approximate chirality, which will ultimately allow us to define topological invariants for



such systems. Let us write a general covariant Hamiltonian  $H_\omega$  on  $\mathbb{C}^{2N} \otimes \ell^2(\mathbb{Z}^d)$  in the grading of  $J$  given in (2.32)

$$H_\omega = \begin{pmatrix} B_\omega & A_\omega^* \\ A_\omega & C_\omega \end{pmatrix}. \quad (2.53)$$

Then the CH is equivalent to saying that the self-adjoint covariant operators  $B_\omega$  and  $C_\omega$  vanish. Given the CH, the BGH is then equivalent to the invertibility of  $A_\omega$ . The invertibility of  $A_\omega$  will turn out to be sufficient to define invariants, so let us state it as a generalization (of a combination of BGH and CA):

**Approximate Chirality Hypothesis (ACH):** *The off-diagonal entry  $A_\omega$  in (2.53) is invertible and, moreover,  $\|B_\omega A_\omega^{-1}\| < 1$  and  $\|C_\omega (A_\omega^*)^{-1}\| < 1$  uniformly in  $\omega$ . The Fermi unitary operator of a Hamiltonian  $H_\omega$  satisfying the ACH is given by  $U_\omega = A_\omega |A_\omega|^{-1}$ .*

Under the ACH, there exists a continuous deformation of Hamiltonians with ACH

$$\lambda \in [0, 1] \mapsto H_\omega(\lambda) = \begin{pmatrix} \lambda B_\omega & A_\omega^* \\ A_\omega & \lambda C_\omega \end{pmatrix}, \quad (2.54)$$

connecting the Hamiltonian  $H_\omega = H_\omega(1)$  to an exact chiral Hamiltonian  $H_\omega(0)$ . Furthermore one has:

**Proposition 2.4.9** *Let  $H_\omega$  satisfy the ACH. Then each operator  $H_\omega(\lambda)$  on the path (2.54) also satisfies the BGH.*

*Proof* The invertibility of  $H_\omega(\lambda)$  is equivalent to the invertibility of

$$H_\omega(\lambda) \begin{pmatrix} 0 & A_\omega^{-1} \\ (A_\omega^*)^{-1} & 0 \end{pmatrix} = \begin{pmatrix} \mathbf{1} & \lambda B_\omega A_\omega^{-1} \\ \lambda C_\omega (A_\omega^*)^{-1} & \mathbf{1} \end{pmatrix},$$

This is guaranteed because the Schur complement  $\mathbf{1} - \lambda^2 B_\omega A_\omega^{-1} C_\omega (A_\omega^*)^{-1}$  is invertible.  $\square$

### 2.4.3 The Half-space and Boundary Hamiltonians

The half-space lattice Hamiltonians are restrictions of the bulk Hamiltonians to the half-space, hence to the Hilbert space  $\mathbb{C}^N \otimes \ell^2(\mathbb{Z}^{d-1} \times \mathbb{N})$ . The surjective partial isometry  $\Pi_d$  from  $\ell^2(\mathbb{Z}^d)$  onto  $\ell^2(\mathbb{Z}^{d-1} \times \mathbb{N})$  will become useful in the following. We want the half-space Hamiltonians to be realistic models of disordered crystals with a *homogeneous* boundary. The latter means that the covariance property w.r.t. magnetic translations along the first  $(d - 1)$ -directions is preserved. For the unitary

class, we claim that this can be achieved within the following generic class of half-space Hamiltonians

$$\hat{H}_\omega = \Pi_d H_\omega \Pi_d^* + \tilde{H}_\omega, \quad (2.55)$$

where the first term represents the restriction of the generic bulk Hamiltonians (2.10) to half-space via a simple Dirichlet boundary condition and the second term will be referred to as the boundary Hamiltonian. Supposing again a finite range condition, its most general covariant expression in the symmetric gauge is

$$\begin{aligned} \tilde{H}_{\text{sym},\omega} &= \sum_{n,m=0}^R \sum_{y \in \mathcal{R}'} \sum_{x \in \mathbb{Z}^{d-1}} \tilde{W}_{n,m}^y(\tau_{x,n}\omega) \otimes |x, n\rangle \langle x, n| U_{\text{sym}}^{y,n-m} \\ &= \sum_{n,m=0}^R \sum_{y \in \mathcal{R}'} \sum_{x \in \mathbb{Z}^{d-1}} e^{\frac{i}{2} \langle y, n-m | \mathbf{B} | x, n \rangle} \tilde{W}_{n,m}^y(\tau_{x,n}\omega) \otimes |x, n\rangle \langle x-y, m|, \end{aligned}$$

where  $\mathcal{R}'$  is a finite subset of  $\mathbb{Z}^{d-1}$ ,  $R$  a finite number and  $\tilde{W}_{n,m}^y \in M_N(\mathbb{C}) \otimes C(\Omega)$ . The representation in the Landau gauge is obtained by conjugating  $\tilde{H}_{\text{sym},\omega}$  with  $e^{\frac{i}{2} \langle X | \mathbf{B}_+ | X \rangle}$ , which gives

$$\tilde{H}_\omega = \sum_{n,m=0}^R \sum_{y \in \mathcal{R}'} \sum_{x \in \mathbb{Z}^{d-1}} e^{\frac{i}{2} \langle y, n-m | \mathbf{B}_+ | y, n-m \rangle} \tilde{W}_{n,m}^y(\tau_{x,n}\omega) \otimes |x, n\rangle \langle x, n| U^{y,n-m}.$$

(2.56)

The Landau gauge representation will be primarily used in the following.

Let us further discuss the terms above. The first term  $\Pi_d H_\omega \Pi_d^*$  models the idealized situation where a boundary was physically created and the remaining hopping matrices are not effected at all by the process of cutting the boundary. Of course, this is not what happens in reality and this is why the boundary Hamiltonian is needed. Note that its hopping matrices depend on  $m$  and  $n$  instead of  $n-m$ , which enables us to model practically any homogeneous distortion occurring near the boundary. These distortions will eventually become experimentally undetectable far away from the boundary, hence we imposed the cut-off at  $m, n \leq R$ , where  $R$  can be arbitrarily large but nevertheless finite.

We now turn our attention to the chiral unitary class. The chiral symmetry on  $\mathbb{C}^{2N} \otimes \ell^2(\mathbb{Z}^{d-1} \times \mathbb{N})$  is given by

$$\hat{J} = \Pi_d J \Pi_d^*. \quad (2.57)$$

Since  $J$  is local,  $\hat{J}$  inherits the basic properties  $\hat{J}^* = \hat{J}$  and  $\hat{J}^2 = \mathbf{1}$ . The bulk-boundary principle derived in our work applies strictly to pairs  $(H, \hat{H})$  of bulk and half-space Hamiltonians which are chiral symmetric with respect to  $(J, \hat{J})$ . The generic half-space Hamiltonians which remains chiral symmetric,  $\hat{J} \hat{H} \hat{J} = -\hat{H}$ ,

takes the form (2.55) with (2.38) and (2.56), and the boundary hopping matrices assume the chiral form

$$\tilde{W}_{n,m}^y(\tau_{x,n}\omega) = \begin{pmatrix} 0 & \tilde{w}_{n,m}^y(\tau_{x,n}\omega) \\ \tilde{w}_{n,m}^y(\tau_{x,n}\omega)^* & 0 \end{pmatrix}. \quad (2.58)$$

For chiral systems, one should also keep in mind the discussion at the end of Sect. 2.3.1 where we have seen that the bulk unit cell needs to be adapted to a given boundary.

We now present the behavior of various quantities of interest. Recall the decomposition Eq. (2.55), which justifies the notation  $\hat{H} = (H, \tilde{H})$  for the covariant families of half-space Hamiltonians. Below, the components  $H$  and  $\tilde{H}$  are assumed of the generic forms (2.12) and (2.56), respectively. When we say that BGH holds for  $\hat{H}$  we are referring specifically to the bulk component  $H$ . The following estimates are by now standard with proofs based on the functional calculus introduced by Dynkin [57], often also referred to as the Helffer-Sjorstrand formula [89].

**Proposition 2.4.10** ([58, 166, 194]) *Assume that the BGH holds for the half-space Hamiltonian  $\hat{H}$ . Then, for any smooth function  $\phi$  with support in the bulk insulating gap,*

$$\sup_{\omega \in \Omega} |\langle x, n | \phi(\hat{H}_\omega) | y, m \rangle| \leq \frac{A_M}{1 + |x - y|^M} e^{-\beta(n+m)}, \quad n, m \in \mathbb{N}, \quad x, y \in \mathbb{Z}^{d-1}.$$

where  $M$  is any integer and  $A_M$  and  $\beta$  are strictly positive constants.

Definition 2.4.5 of continuous deformations extends literally to the half-space Hamiltonians. By similar proofs, one obtains the following:

**Proposition 2.4.11** ([58, 166, 194]) *Let  $\hat{H}(t)$  be a continuous deformation of a family of covariant half-space Hamiltonians. Then, for any smooth function  $\phi$  with support in a common insulating gap,*

$$\sup_{\omega \in \Omega} |\langle x, n | \phi(\hat{H}_\omega(t)) - \phi(\hat{H}_\omega(t')) | y, m \rangle| \leq \frac{C_M(t, t')}{1 + |x - y|^M} e^{-\beta(n+m)},$$

where  $M$  is any integer,  $\beta$  is a strictly positive constant, and  $C_M(t, t')$  is a continuous function of the arguments such that  $C_M(t, t) = 0$  for all  $t \in [0, 1]$ .

Bulk and Boundary Invariants for Complex Topological  
Insulators

From K-Theory to Physics

Prodan, E.; Schulz-Baldes, H.

2016, XXII, 204 p. 1 illus., Hardcover

ISBN: 978-3-319-29350-9